

DNA metabarcoding reveals vertical variation and hidden diversity of Alveolata and Rhizaria communities in the western North Pacific

メタデータ	言語: en 出版者: 公開日: 2022-10-03 キーワード (Ja): キーワード (En): 作成者: 寒川, 清佳, ナカムラ, ヤスヒデ, 長井, 敏, ニシ, ノリコ, 日高, 清隆, 瀬藤, 聡 メールアドレス: 所属: 水産研究・教育機構, 島根大学, 水産研究・教育機構, AXIOHELIX Co. Ltd, 水産研究・教育機構, 水産研究・教育機構
URL	https://fra.repo.nii.ac.jp/records/100

This work is licensed under a Creative Commons Attribution-NonCommercial-ShareAlike 3.0 International License.



Highlights

- Eukaryotic community zoned vertically, Kuroshio epi-, NPIW meso- and bathypelagic.
- Eukaryotic plankton diversity was remarkably low in the NPIW.
- Collodaria, Syndiniales and Oligohymenophorea were predominant in the NPIW.
- Acantharia, Nassellaria, Spumellaria and Phaeodaria OTUs peaked at 100 m depth.
- Taxopodia, Nassellaria and “Other Cercozoa” reads peaked in the deepest layer.

1 **1 DNA metabarcoding reveals vertical variation and hidden diversity of Alveolata and**

2 **2 Rhizaria communities in the western North Pacific**

3 **3**

4 **4 Sayaka Sogawa^{a,*}, Yasuhide Nakamura^b, Satoshi Nagai^a, Noriko Nishi^c, Kiyotaka Hidaka^a, Yugo**

5 **5 Shimizu^a, and Takashi Setou^a**

6 **6**

7 **7 ^a Fisheries Resources Institute, Japan Fisheries Research and Education Agency, Yokohama,**

8 **8 Kanagawa, Japan**

9 **9 ^b Shimane University, Estuary Research Center, 1060, Nishikawatsu-cho, Matsue, Shimane 690-**

10 **10 8504, Japan**

11 **11 ^c AXIOHELIX Co. Ltd, 1-12-17 Kandaizumicho, Chiyoda-ku, Tokyo 101-0024, Japan**

12 **12**

13 **13 * Corresponding author. Fisheries Resources Institute, Japan Fisheries Research and Education**

14 **14 Agency, 2-12-4 Fukuura, Kanazawa, Yokohama, Kanagawa 236-8648, Japan.**

15 **15 *E-mail address:* ssogawa@affrc.go.jp (S. Sogawa).**

16 **16**

1
2
3 **17 ABSTRACT**
4

5 **18** Metabarcoding technology using high-throughput sequencing has revolutionized the current
6
7
8 **19** understanding of the diversity and ecology of eukaryotic microorganisms. The aim of the present
9
10
11 **20** study was to investigate vertical and seasonal variation in eukaryotic plankton communities and
12
13
14 **21** to assess the diversity of eukaryotic plankton, using 18S rRNA sequencing, over a depth gradient
15
16
17 **22** in subtropical waters affected by the Kuroshio Current. In particular, the present study focused
18
19 **23** on the diversity and ecology of Alveolata and Rhizaria taxa, which include a variety of plankton
20
21
22 **24** species with fragile skeletons or soft bodies. Three vertically distinct eukaryotic communities
23
24
25 **25** were identified: the Kuroshio-influenced epipelagic zone (<200 m), the North Pacific
26
27 **26** Intermediate Water (NPIW)-dominated mesopelagic zone (500–1000 m), and the bathypelagic
28
29
30 **27** zone (2000–3000 m). The operational taxonomic unit (OTU) richness was greatest near the
31
32
33 **28** surface (<200 m depth), gradually decreasing with increasing depth, and lowest in deeper layers,
34
35
36 **29** and OTU diversity (Pielou’s evenness and Shannon-Wiener diversity indices) were lowest in the
37
38
39 **30** mesopelagic layer (500–1000 m depth). Hidden diversity was observed in both groups in both the
40
41
42 **31** surface and deeper layers of the western North Pacific, as well as in the NPIW, which was
43
44
45 **32** characterized by the lowest salinity and oxygen concentrations in the study area. In the NPIW,
46
47
48 **33** the Rhizaria yielded relatively more sequence reads than other taxa. Furthermore, specific taxa,
49
50
51 **34** such as Collodaria (Radiolaria), Syndiniales (dinoflagellates), and Oligohymenophorea (ciliates),
52
53
54 **35** were predominant, according to OTU richness and the relative abundance of sequence reads.
55
56
57 **36** These findings indicate that a unique ecosystem was formed over time in the NPIW-isolated water
58
59
60 **37** mass.
61
62
63
64
65

1
2
3
4
5
6
7
8
9
10
11
12
13
14
15
16
17
18
19
20
21
22
23
24
25
26
27
28
29
30
31
32
33
34
35
36
37
38
39
40
41
42
43
44
45
46
47
48
49
50
51
52
53
54
55
56
57
58
59
60
61
62
63
64
65

39 *Key words:*

40 Kuroshio

41 Eukaryotic plankton

42 Unicellular zooplankton

43 18S rRNA

44 Diversity

45

46 Abbreviations: NPIW, North Pacific Intermediate Water; OTU, operational taxonomic

47 unit

48

1
2
3 **49 1 Introduction**
4

5
6 **50** The Kuroshio Current is a warm ocean current that transfers heat and a diverse array of organisms
7
8 **51** to the high latitudes of the central North Pacific, and because many fish species spawn and migrate
9
10
11 **52** in the surrounding areas, the current substantially influences the ecosystem structure and fisheries
12
13 **53** in East Asia (Barkley, 1970; Qiu and Lukas, 1996; Imasaki et al., 2001; Sassa et al., 2008;
14
15 **54** Morimoto, 2010; Sugisaki et al., 2010; Harris and Lang, 2014; Yamazaki et al., 2016; Nagai et
16
17 **55** al., 2019; Kobari et al., 2020). Marine ecosystems are based on primary production by
18
19 **56** phytoplankton and bacterial plankton, and the energy and organic materials that these organisms
20
21
22 **57** produce are transferred to higher-trophic-level organisms, such as fishes, through intermediates,
23
24
25 **58** like heterotrophic plankton, that consume primary producers. Therefore, it is essential to elucidate
26
27
28 **59** the dynamics of lower trophic levels in the Kuroshio ecosystem, which is significant in terms of
29
30
31 **60** oceanography and fisheries, and to monitor its continuous changes.
32
33

34
35 **61** Even though a large proportion of plankton species are protists (i.e., eukaryotic,
36
37 **62** predominantly single-celled organisms), most *in situ* studies of plankton communities have
38
39
40 **63** focused on relatively large zooplankton, such as crustaceans, or phytoplankton, such as diatoms,
41
42
43 **64** which can be identified using microscopy. Moreover, marine plankton are highly diverse, and
44
45
46 **65** advanced techniques are often required for morphological identification. Advances in molecular
47
48
49 **66** biological techniques, such as DNA metabarcoding using high-throughput sequencing, have
50
51
52 **67** enabled researchers to investigate the structures of plankton communities that contain small and
53
54
55 **68** amorphous plankton species (Countway et al., 2007; Schnetzer et al., 2011; Hu et al., 2016;
56
57
58 **69** Pernice et al., 2016; Ruppert et al., 2019; Canals et al., 2020; Brisbin et al., 2020; Ollison et al.,
59
60
61 **70** 2021). Metabarcoding has also become a powerful and efficient tool for monitoring and detecting
62
63
64
65

1
2
3 71 hidden diversity, with community-wide taxonomic coverage (Lindeque et al., 2013; Mohrbeck et
4
5 72 al., 2015; Valentini et al., 2016; Hirai et al., 2017; Ruppert et al., 2019; Suter et al., 2020). The
6
7
8 73 taxonomic identification of Alveolata and Rhizaria, which contain many species with fragile
9
10
11 74 skeletons (e.g., radiolarians) or soft bodies (e.g., ciliates), using morphological techniques has
12
13
14 75 always been considered difficult. Recent DNA metabarcoding studies have revealed that
15
16 76 Alveolata and Rhizaria are highly diverse and contribute significantly to ecological processes,
17
18
19 77 such as vertical exports and trophic transfers, in marine ecosystems (Bescot et al., 2016;
20
21 78 Gutierrez-Rodriguez et al., 2019; Preston, 2019).

22
23
24 79 The structures of Alveolata and Rhizaria communities are drastically affected by depth
25
26
27 80 and season (Not et al., 2007; Nakamura et al., 2013). In the areas surrounding the Kuroshio
28
29
30 81 Current, the environmental conditions of the marine environment vary both horizontally and
31
32 82 vertically (Kuroda et al., 2018; Yasuda, 2003; Miyazawa et al., 2009). Thus, community structure
33
34
35 83 may be significantly affected by environmental change. A study that used 18S rRNA sequencing
36
37 84 to investigate the eukaryotic plankton community of coastal waters affected by the Kuroshio
38
39
40 85 Current reported diverse assemblages of diatoms and dinoflagellates (Kok et al., 2012), and a
41
42
43 86 more recent study, which also investigated eukaryotic plankton communities using 18S rRNA,
44
45 87 reported finding three distinct communities (coastal, Kuroshio, and mixed water) within the
46
47
48 88 surface layer of the northwestern Pacific (Wu et al., 2020). Meanwhile, Endo and Suzuki (2019),
49
50
51 89 who surveyed the surface layer, reported that diatoms and haptophytes were more diverse in the
52
53
54 90 Kuroshio axis. Furthermore, a water mass called the North Pacific Intermediate Water (NPIW) is
55
56 91 formed in the mixed water region between the Oyashio and Kuroshio waters in the western North
57
58
59 92 Pacific and is widely distributed in subtropical North Pacific waters between the surface and deep
60
61
62
63
64
65

1
2
3 93 layers and between 20 and 45°N (Sverdrup et al., 1942; Talley, 1993; Yasuda, 1997; Masujima
4
5 94 et al., 2003; Shimizu et al., 2004). Most studies of plankton in the NPIW have focused on
6
7
8 95 foraminiferans or large gelatinous zooplankton (Ortiz et al., 1996; Morita et al., 2017), and the
9
10
11 96 comprehensive plankton community structure, especially in the southern portions of the NPIW,
12
13
14 97 has yet to be reported.

15
16 98 The aim of the present study was to investigate the eukaryotic plankton communities
17
18 99 in subtropical waters, in which epipelagic and mesopelagic layers are associated with different
19
20
21 100 water bodies (the Kuroshio Current and NPIW, respectively). Year-round seasonal surveys of
22
23
24 101 marine plankton and physicochemical environmental parameters at different depths (5–3000 m)
25
26
27 102 were conducted at several sites along a transect across Kuroshio, and 18S rRNA (V7–9) DNA
28
29 103 metabarcoding was used to assess the dynamics and diversity of eukaryotic plankton communities.

30
31
32 104

33
34
35 105

36 37 106 **2 Material and methods**

38 39 107 *2.1 Sampling locations*

40
41
42 108 Sampling was conducted from aboard the *R/V Soyo-Maru* (National Research Institute of
43
44
45 109 Fisheries Science, Japan Fisheries Research and Education Agency) in the northwestern Pacific,
46
47
48 110 south of Japan, adjacent to the Kuroshio Current (Fig. 1). A total of 110 samples were collected
49
50
51 111 from different depths (from 5 or 10 m to 3000 m) during five cruises that were conducted from
52
53
54 112 August 2015 to August 2016 (Table 1), and the locations of sampling stations were selected in
55
56 113 order to establish a transect that crossed the Kuroshio Current axis at 138°E (Fig. 1). The sampling
57
58 114 sites were designated as northern (north of Kuroshio), middle (Kuroshio axis, but later found to

1
2
3
4
5
6
7
8
9
10
11
12
13
14
15
16
17
18
19
20
21
22
23
24
25
26
27
28
29
30
31
32
33
34
35
36
37
38
39
40
41
42
43
44
45
46
47
48
49
50
51
52
53
54
55
56
57
58
59
60
61
62
63
64
65

115 be off-axis), or southern (south of Kuroshio), and the location of the Kuroshio Current axis was
116 determined using hydrographic condition images based on data from vessels, satellites, and Japan
117 Meteorological Agency products, which were published by the fisheries research institutes of
118 Tokyo, Chiba, Kanagawa, Shizuoka, Mie and Wakayama prefectures (provided on website of
119 Kanagawa Prefectural Fisheries Technology Center; Fig. 1).

120

121 *2.2 Seawater sampling and processing*

122 Vertical temperature and salinity profiles were measured continuously using a conductivity-
123 temperature-depth (CTD) sensor (SBE 911plus; Seabird Co.). Seawater samples for generating
124 discrete vertical profiles of nutrients (nitrate+nitrite, silica, and phosphate) and chlorophyll *a*
125 concentrations were collected at several depths using Niskin bottles mounted to the rosette
126 carrying the CTD sensor. For DNA metabarcoding analysis, seawater samples (1 L) were passed
127 through Nucleopore membrane filters (0.2 μ m), and stored at -30°C until the DNA extraction.
128 DNA was extracted using 5% Chelex buffer, as described previously (Nagai et al., 2012; Tanabe
129 et al., 2016). For chlorophyll *a* analysis, seawater samples (300 mL) were filtered onto Whatman
130 GF/F filters, extracted using 6 mL of *N,N*-dimethylformamide (DMF), and analyzed by applying
131 the fluorometric Welschmeyer method. Seawater samples for chlorophyll *a* and nutrient analysis
132 were stored at -30°C until nutrient and chlorophyll concentrations were measured using a flow
133 injection analyzer (TrAAcs 2000; Bran + Luebbe) and a fluorometer (10-AU; Turner Designs,
134 Inc.), respectively.

135

1
2
3
4
5
6
7
8
9
10
11
12
13
14
15
16
17
18
19
20
21
22
23
24
25
26
27
28
29
30
31
32
33
34
35
36
37
38
39
40
41
42
43
44
45
46
47
48
49
50
51
52
53
54
55
56
57
58
59
60
61
62
63
64
65

136 *2.3 DNA sequence generation and processing*

137 Metagenomic analysis was performed using the MiSeq 300PE platform (Illumina, San Diego, CA,
138 USA) and universal primers (SSR-F1289-sn, F: TGGAGYGATHTGTCTGGTTDATTCCG;
139 SSR-R1772-sn, R: TCACCTACGGAWACCTTGTTACG; Sildever et al., 2019), which were
140 designed to amplify the V7–9 hypervariable regions of the 18S-rRNA gene. A massively parallel
141 paired-end sequencing workflow was designed by consulting the Illumina document (Illumina,
142 2013). Two-step PCR was used to construct paired-end libraries (Sildever et al., 2019), and the
143 resulting PCR products were quantified, pooled in equal concentrations, and stored at -30°C until
144 sequenced using the MiSeq Reagent Kit v3 (2 × 300 bp; Illumina).

145
146 *2.4 Metabarcoding data treatment processes and operational taxonomic unit picking*

147 Nucleotide sequences were demultiplexed using the 5-multiplex identifier tags and primer
148 sequences. Sequences that contained palindromes of >30 bp and homopolymers of >9 bp were
149 trimmed at both ends. The 30 tails with mean quality scores of <30 at the end of the last 25-bp
150 window and 50 and 30 tails with mean quality scores <20 at the end of the last window were also
151 removed. Sequences longer than 300 bp were truncated to 300 bp by trimming 30 tails, and
152 sequences shorter than 250 bp were filtered out. Both demultiplexing and trimming were
153 performed using Trimmomatic version 0.35 (<http://www.usadellab.org/cms/?page=trimmomatic>).

154 The trimmed and filtered sequences were merged into paired reads using Usearch
155 version 8.0.1517 (<http://www.drive5.com/usearch/>). After singletons were removed, the
156 remaining sequences were aligned using Clustal Omega version 1.2.0.
157 (<http://www.clustal.org/omega/>). Multiple sequences were aligned, and only sequences that were

1
2
3
4
5
6
7
8
9
10
11
12
13
14
15
16
17
18
19
20
21
22
23
24
25
26
27
28
29
30
31
32
33
34
35
36
37
38
39
40
41
42
43
44
45
46
47
48
49
50
51
52
53
54
55
56
57
58
59
60
61
62
63
64
65

158 contained more than 75% of the read positions were extracted. Filtering and part of the multiple-
159 alignment process were performed using the *screen.seqs* and *filter.seqs* commands in Mothur, as
160 described in the MiSeq standard operating procedure (http://www.mothur.org/wiki/MiSeq_SOP;
161 Schloss et al., 2011), and erroneous and chimeric sequences were detected and removed using the
162 *pre.cluster (diffs=4)* and *chimera.uchime (minh=0.1)* commands in Mothur, respectively
163 (http://drive5.com/usearch/manual/uchime_algo.html; Edgar et al., 2011).

164 The sequence data were divided into several groups and treated separately, owing to
165 the limited memory capacity of the server. The FASTA file (*result.fasta*) of each group was
166 merged, and identical sequences were collated into operational taxonomic units (OTUs) using the
167 *unique.seqs* command in Mothur. Because representative sequences from different Miseq runs
168 could contain identical sequences, the sequences were clustered to re-select representative
169 sequences at a 0.99 level of sequence identity using CD-HIT-EST version 4.6.8 (Li and Godzik,
170 2006) with command-line parameters '*-c 0.99 -n 11 -d 0 -p 1*'. Representative sequences, which
171 were designated as OTUs, were counted using the *count.seqs* command, and sequences clustered
172 into OTUs between different runs were counted by referring to both *count.seqs* and CD-HIT data.
173 These sequences were used for subsequent taxonomic identification analyses, and demultiplexed
174 and filtered, but untrimmed, sequence data were deposited into the DDBJ Sequence Read Archive
175 (access no. DRA010320).

176

177 *2.5 OTU identification*

178 To taxonomically identify the selected OTUs, a subset of nucleotide databases that satisfied the
179 chosen conditions (described below) were prepared for BLAST analysis. One keyword was

1
2
3
4
5
6
7
8
9
10
11
12
13
14
15
16
17
18
19
20
21
22
23
24
25
26
27
28
29
30
31
32
33
34
35
36
37
38
39
40
41
42
43
44
45
46
47
48
49
50
51
52
53
54
55
56
57
58
59
60
61
62
63
64
65

180 selected from among “ribosomal,” “rrna,” and “rdna,” but “protein” protein was not included in
181 the title. For the taxonomy search, the keywords “metagenome,” “uncultured,” and
182 “environmental” were not included. The sequences of retrieved GenBank IDs from the nucleotide
183 database downloaded from the NCBI FTP server on March 22, 2019, were used to construct a
184 reference sequence database.

185 Each OTU was then identified by BLAST search (Cheung et al., 2010) using NCBI
186 BLAST+ 2.2.30+ (Camacho et al., 2009), with the default parameters, and nucleotide subset
187 described above as the database. For each query sequence, taxonomic information was obtained
188 from BLAST hits with the highest bitscores, and OTUs with the same top hit were merged. When
189 an OTU matched several data points with the same bitscore and top hit similarity, the OTUs were
190 merged. Therefore, in some cases, several data were merged in a single OTU. Because the
191 removal of error-containing sequences was imperfect and error-containing sequences remained
192 in the dataset, error-containing sequences were detected as artificial OTUs with the same top
193 BLAST hit name but with slight differences. To avoid the overestimation of OTU richness,
194 artificial OTUs were merged and represented by the OTU with the highest similarity score. One
195 OTU with abnormally high read numbers was excluded from data analysis because it was thought
196 to contain chimeric sequences.

197

198 *2.6 Data analysis*

199 All multivariate analyses of plankton community structure and diversity were performed using
200 PRIMER version 7 with the PERMANOVA+ add-on software (Anderson et al., 2008; Clarke and
201 Gorley, 2015). For multivariate analyses, Bray-Curtis similarity among samples was calculated

1
2
3
4
5
6
7
8
9
10
11
12
13
14
15
16
17
18
19
20
21
22
23
24
25
26
27
28
29
30
31
32
33
34
35
36
37
38
39
40
41
42
43
44
45
46
47
48
49
50
51
52
53
54
55
56
57
58
59
60
61
62
63
64
65

202 using log-transformed sequence abundance data. Non-metric multidimensional scaling ordination
203 was used to visualize differences between the plankton communities of seawater samples, and
204 similarity analysis was used to identify differences between samples collected at different depths
205 or during different months (Clarke, 1993). To investigate the effects of environmental variables
206 on Alveolata and Rhizaria communities, multicollinearity was addressed by removing variables
207 with correlations of >0.95, and the data were processed using distance-based linear modeling
208 (DistLM) and redundancy analysis (dbRDA). Plankton diversity was assessed by calculating
209 richness (number of OTUs), Shannon-Wiener diversity (Shannon and Weaver, 1949), and
210 evenness (Pielou, 1966).

211
212

213 **3 Results**

214 *3.1 Physical and chemical characteristics of the water masses*

215 Environmental variation was observed among the sampling areas, northern sites, and southern
216 sites of each cruise (Fig. 2 and Fig. S1). Vertical mixing in the surface layer was observed in
217 March (up to ~100 m at the northern site and ~200 m at the southern site; Fig. 2). The maximum
218 salinity was observed in the surface layer, whereas the salinity minimum layers were observed at
219 750–1000 m in the southern sites and 300–500 m in the northern and middle sites (Fig. 2). A
220 potential density of 26.8 σ_θ (range: 26.6–26.9 σ_θ), which indicated NPIW, was also observed at
221 the salinity minimum layers (Fig. 2). Oxygen decreased with increasing depth, and oxygen
222 minimum layers were observed just below the salinity minimum layers (1250 and 750–1000 m at
223 the southern and northern sites, respectively; Fig. 2). In contrast to oxygen levels, nutrient

1
2
3 224 (nitrate+nitrite, silica, and phosphate) concentrations increased with increasing depth (Fig. S1),
4
5 225 and maximum nitrate+nitrite and phosphate concentrations were observed in the oxygen
6
7
8 226 minimum layers (Fig. S1).
9

10
11 227

12
13 228 *3.2 Eukaryotic plankton community structure and diversity*
14
15

16 229 The present study detected a total of 1956 OTUs of oceanic plankton, including 872 OTUs
17
18 230 attributed to supergroup Alveolata, which was represented by dinoflagellates and ciliates; 202
19
20
21 231 OTUs attributed to Rhizaria, which was represented by radiolarians and cercozoans; 275 OTUs
22
23
24 232 attributed to Opisthokonta, which was represented by metazoans and fungi; 323 OTUs attributed
25
26
27 233 to Stramenopiles, which was represented by diatoms; and 133 OTUs attributed to Archaeplastida
28
29 234 (Fig. 3). Alveolata accounted for the largest proportion (nearly half) of all OTUs, and Rhizaria
30
31
32 235 and Alveolata accounted for 33 and 40% of all sequence reads, respectively (Fig. 3).
33

34 236 Non-metric multidimensional scaling ordination and analysis of similarity revealed
35
36
37 237 significant differences in oceanic plankton communities with respect to water depth (global
38
39
40 238 $R=0.751$, $p=0.001$, no. permutations=999; Fig. 4). Pairwise tests revealed significant differences
41
42
43 239 between shallow and deep communities (Table 2). There were significant differences ($R=0.92-1$,
44
45 240 $p=0.001$) between communities from surface layers (5–10, 50, and 100 m) and deeper layers (500,
46
47
48 241 1000, 2000, and 3000 m) and small differences (highly overlapped) between communities
49
50
51 242 collected at 5, 10, and 50 m ($R=0.13$, $p=0.009$), 500 and 1000 m, and 2000 and 3000 m ($R=0.18-$
52
53 243 0.22 , $p=0.001$). However, no significant differences were detected in the plankton communities
54
55
56 244 collected during different months (global $R=0.031$, $p>0.05$; pairwise tests $R<0.07$, $p>0.05$, no.
57
58 245 permutations=999).
59
60
61
62
63
64
65

1
2
3 246 More OTUs were detected in surface layers (<200 m depth) than in deeper layers (>200
4
5 247 m depth), however, other diversity measures failed to decrease with increasing depth that Pielou's
6
7
8 248 evenness was higher at 2000 and 3000 m but lower at 500 and 1000 m, and Shannon-Wiener
9
10
11 249 diversity was higher in surface layers but lower at 500 and 1000 m (Fig. 5). The mean number of
12
13
14 250 OTUs for most groups, including Alveolata, Archaeplastida, Excavata, Haptophyta, Opisthokonta,
15
16 251 and Stramenopiles, were consistently low in deep layers and were three to 19 times higher in
17
18
19 252 surface layers. However, the richness of Rhizaria peaked at 100 m (41 OTUs; Fig. 6a). The
20
21
22 253 proportion of sequence reads attributed to Alveolata was relatively constant (35–45%), regardless
23
24 254 of depth, whereas the proportions attributed to Opisthokonta and Archaeplastida were higher at
25
26
27 255 depths of <100 m, and the proportion attributed to Rhizaria was higher at depths of >100 m,
28
29
30 256 especially at 500 and 1000 m (Fig. 6b).

31
32 257

33 34 258 *3.3 Alveolata and Rhizaria communities*

35
36
37 259 Among the Alveolata taxa, dinoflagellates (i.e., Dinoflagellata) represented the largest number of
38
39
40 260 OTUs (659) and proportion of sequence reads (91.6%), followed by ciliates (i.e., Ciliophora; 167
41
42
43 261 OTUs and 5.4% of sequence reads; Fig. 7). Among the dinoflagellates, Gymnodiniales,
44
45
46 262 Syndiniales, and Peridinales accounted for relatively high proportions of sequence reads (32.9,
47
48 263 29.2, and 19.5%, respectively; Fig. 7), and Peridinales and Gymnodiniales also accounted for
49
50
51 264 relatively large numbers of OTUs (240 and 152, respectively; Fig. 7). Among the ciliates,
52
53
54 265 Oligohymenophorea and Oligotrichia accounted for relatively high proportions of sequence reads
55
56 266 (45.7 and 27.1%, respectively) and numbers of OTUs (27 and 66, respectively; Fig. 7).

1
2
3 267 Among the Rhizaria taxa, Radiolaria and Cercozoa accounted for nearly half of all
4
5 268 OTUs (111 and 90 OTUs, respectively; Fig. 8), and no OTUs were attributed to Foraminifera,
6
7
8 269 which is another major group in Rhizaria. Among Radiolaria, Spumellaria accounted for the
9
10
11 270 greatest number of OTUs (n=37), followed by Acantharia (34 OTUs), Collodaria (24 OTUs),
12
13 271 Nassellaria (12 OTUs), and Taxopodia (4 OTUs; Fig. 8). However, for Cercozoa, most OTUs
14
15
16 272 were categorized as “Other Cercozoa” (86 OTUs, 95.6%), and the remaining four were attributed
17
18
19 273 to Phaeodaria (4.4%; Fig. 8). Radiolaria accounted for most of the sequence attributed to Rhizaria
20
21 274 (97.2%), whereas Cercozoa accounted for only 2.8% (Fig. 8), and among the Radiolaria sequence
22
23
24 275 reads, Collodaria accounted for the highest proportion (48.7%), followed by Taxopodia (20.6%),
25
26
27 276 Acantharia (15.0%), Spumellaria (12.7%), and Nassellaria (3.1%; Fig. 8). For the Cercozoa
28
29 277 sequence reads, “Other Cercozoa” accounted for the highest proportion (93.7%), and Phaeodaria
30
31
32 278 accounted for only 6.3% (Fig. 8).

33
34
35 279 Cluster analysis classified the 110 Alveolata community samples into two large
36
37 280 clusters, the surface layer (<200 m) and deeper layer (>200 m) at 29% similarity, accordingly to
38
39
40 281 the similarity profile test (SIMPROF; Clarke, 1993), and the 110 Rhizaria community samples
41
42
43 282 into three large clusters, the surface layer (<200 m), mainly composed of samples from 50 m and
44
45 283 100 m layers (with one 500 m layer sample), and a deeper layer (>200 m), at 22.5 and 37%
46
47
48 284 similarities based on the SIMPROF test (Fig. 9). Further community structure analysis was
49
50
51 285 conducted each on the surface layer (<200 m) and the deeper layer (>200 m), and only surface
52
53
54 286 layer communities showed significant differences between sampling months: March vs. other
55
56 287 months (ANOSIM pairwise test, R=0.40–0.57, p=0.001) for the Alveolata community and March

1
2
3
4
5
6
7
8
9
10
11
12
13
14
15
16
17
18
19
20
21
22
23
24
25
26
27
28
29
30
31
32
33
34
35
36
37
38
39
40
41
42
43
44
45
46
47
48
49
50
51
52
53
54
55
56
57
58
59
60
61
62
63
64
65

288 vs. August (both 2015 and 2016; ANOSIM pairwise test, $R=0.44-0.47$, $p=0.001$) for the Rhizaria
289 community.

290 DistLM analysis revealed significant associations between both the Alveolata and
291 Rhizaria communities and the ten (<200 m) or eight (>200 m) of the tested environmental
292 variables (Table 3). One variable (phosphate concentration) was excluded prior to analysis of
293 surface layer communities because it was strongly correlated ($|r|>0.95$) with both nitrate+nitrite
294 and silica, and two variables (phosphate and silica) were excluded from analysis of deeper layer
295 communities because they were strongly correlated with nitrate+nitrite ($|r|>0.95$). In the marginal
296 tests of DistLM analysis, depth, temperature, nitrate+nitrite, and silica individually explained
297 10.4–13.3% of variation in surface layer Alveolata community structure, and depth, temperature,
298 and salinity individually explained 8.1–10.7% of variation the deeper layer Alveolata community
299 structure (Table 3). Meanwhile, depth, temperature, nitrate+nitrite, and chllophyll *a* individually
300 explained 8.2–16.5% of variation in the surface layer Rhizaria community structure, and depth,
301 temperature, and salinity individually explained 12.8–16.7% of variation in the deeper layer
302 Rhizaria community structure (Table 3).

303 For the Alveolata community structure, the first two dbRDA axes explained 65.5 and
304 24.1% of the fitted and total variation in the surface layer, respectively, and 68.2 and 15.3% of
305 the fitted and total variation in the deeper layer. For the Rhizaria community structure, the first
306 two dbRDA axes explained 76.1 and 31.1% of the fitted and total variation in the surface layer,
307 respectively, and 76.7 and 22.2% of the fitted and total variation in the deeper layer. In the analysis
308 of surface layer Alveolata and Rhizaria communities, vector overlay indicated that axis 1 was
309 strongly correlated with depth and that axis 2 was strongly correlated with month, whereas in the

1
2
3
4
5
6
7
8
9
10
11
12
13
14
15
16
17
18
19
20
21
22
23
24
25
26
27
28
29
30
31
32
33
34
35
36
37
38
39
40
41
42
43
44
45
46
47
48
49
50
51
52
53
54
55
56
57
58
59
60
61
62
63
64
65

310 analysis of deeper layers, axis 2 was strongly correlated with temperature and nitrate+nitrite for
311 the Alveolata community and with temperature for the Rhizaria community (Fig. 9). In addition
312 to depth, season was also a variation factor for Alveolata and Rhizaria communities in the surface
313 layer.

314 The mean OTU richness and sequence read proportions of Alveolata at different depths
315 were compared with respect to class and order (Figs. S2 and S3). Most Alveolata taxa yielded
316 greater OTU richness in surface layers, although Syndiniales OTUs were more evenly distributed
317 and peaked at 500 m (Fig. S2). The proportions of sequence reads of some dinoflagellates (i.e.,
318 Gymnodinales, Peridinales, Coccidinales, Prorocentrales, and Gonyaulacales), ciliates (i.e.,
319 Oligotrichia, Mesodinea, and Nassophorea), and Apicomplexa in surface layers gradually
320 decreased with increased depth, to 1000 m depth, and then increased at 2000 and 3000 m (Fig.
321 S3), whereas proportions of sequence reads for both Syndiniales (dinoflagellates) and
322 Oligohymenophorea (ciliates) peaked at both 500–1000 m depths (Fig. S3).

323 Mean numbers of Acantharia, Nassellaria, Spumellaria, and Phaeodaria OTUs peaked
324 at 100 m depth, whereas Collodaria OTUs peaked at 500 m depth (Fig. S4). The mean number of
325 Collodaria OTUs was relatively low in the upper layer, whereas the number of ‘Other Cercozoa’
326 OTUs decreased gradually from the surface layers to the deeper layers. The vertical dynamics of
327 Acantharia, Nassellaria, and Spumellaria OTU number in the present study suggests that these
328 groups are more diverse in surface layers than in deeper layers. The proportions of Acantharia,
329 Nassellaria, Taxopodia, and “Other Cercozoa” sequence reads peaked at 2000 or 3000 m (Fig.
330 S5). Meanwhile, the proportion of Collodaria sequence reads peaked at 500 m, and similar to
331 Collodaria OTU numbers, the mean proportions of sequence reads were relatively small at 5–10,

1
2
3 332 50, and 100 m. In contrast, proportion of Phaeodaria OTUs and sequence reads peaked at 50 and
4
5 333 100 m, respectively.
6

7
8 334
9

10
11 335
12

13 336 **4 Discussion**
14

15
16 337 The present study revealed that there are clear differences in the community structure and
17
18 338 diversity of eukaryotic plankton found at different depths and in different water masses in the
19

20
21 339 western North Pacific. The eukaryotic plankton community differed distinctly between the
22

23
24 340 epipelagic layer (<200 m), which was strongly influenced by the Kuroshio Current, and deeper
25

26
27 341 layers (>200 m). These findings are similar to those of a study conducted in the Atlantic, which
28

29
30 342 also reported distinct protistan assemblages in the euphotic zone and deep sea and a vast diversity
31

32
33 343 of Alveolata and Rhizaria (Countway et al., 2007; Not et al., 2007). In addition, the present study
34

35
36 344 also noted a significant difference in the eukaryotic plankton communities of the mesopelagic
37

38
39 345 layer (500–1000 m) and bathypelagic layer (2000–3000 m). In general, the plankton community
40

41
42 346 varied in accordance with vertical changes in environmental conditions. For example, nutrient
43

44
45 347 concentrations and salinity increased with increasing depth, and temperature and chlorophyll
46

47
48 348 concentration decreased with increasing depth. However, diversity did not exhibit a linear
49

50
51 349 gradient with depth. The number of OTUs was greatest in the surface layer (<200 m depth),
52

53
54 350 decreasing with increasing depths, and lowest in the deepest layer (3000 m), whereas the diversity
55

56
57 351 indexes (Pielou's evenness and Shannon-Wiener diversity index) were remarkably low in the
58

59
60 352 mesopelagic layers (500–1000 m depth), where the NPIW water mass was distributed (Reid,
61

62
63 353 1965; Sverdrup et al., 1942). The NPIW is formed in the mixed water region between the
64
65

1
2
3
4
5
6
7
8
9
10
11
12
13
14
15
16
17
18
19
20
21
22
23
24
25
26
27
28
29
30
31
32
33
34
35
36
37
38
39
40
41
42
43
44
45
46
47
48
49
50
51
52
53
54
55
56
57
58
59
60
61
62
63
64
65

354 Kuroshio Extension and the Oyashio Front in the western North Pacific and spreads southward
355 (Talley, 1993; Watanabe et al., 1995). The plankton community structures of the Oyashio and
356 Kuroshio water areas are distinct, and the plankton community of the nutrient-rich Oyashio area
357 is generally characterized by fewer species (lower diversity) and higher abundance, whereas the
358 plankton community in the nutrient-poor Kuroshio area is characterized by more species (higher
359 diversity) and lower abundance (Sogawa et al., 2013; Morita et al., 2017; Ohtsuka and Nishida,
360 2017; Matsumoto and Yamaguchi, 2020). A study that used a video plankton recorder reported
361 that Hydrozoa, Ctenophora, Copepoda, and Rhizaria were most abundant within the NPIW and
362 emphasized that radiolarians may have physically accumulated in the water mass (Ichikawa,
363 2008; Ichikawa et al., 2007). The estimated residence time of NPIW, which spreads southward to
364 Japan, is 20 years, with a subsequent increase in salinity and reduction of oxygen (Shimizu et al.,
365 2004; Talley, 1993; Talley et al., 1995). The low mesopelagic diversity in the study area could be
366 due to the special formation process and environmental characteristics (salinity minimum and
367 oxygen minimum) of the NPIW and long residence time that maintains a uniform environment.
368 These results suggest that unique isolated ecosystems form over time in NPIW. For example,
369 several radiolarian species were detected almost exclusively in the NPIW (e.g., *Collophidium*
370 *ovatum*, *Thalassicolla pellucida*, and *Thalassicolla melacapsa*, Collodaria). Furthermore,
371 Collodaria, which include a large number of mixotrophs that harbor algal symbionts, are
372 frequently reported in the surface layers (Biard et al., 2016; Nakamura et al. 2019; Suzuki and
373 Not, 2015), even though they retain high species diversity in both mesopelagic and deep layers
374 (Biard et al., 2015; Pernice et al., 2016). In the present study, the OTU and sequence read numbers
375 attributed to Order Collodaria were highest in the NPIW, whereas Order Orodaria, which is

1
2
3
4
5
6
7
8
9
10
11
12
13
14
15
16
17
18
19
20
21
22
23
24
25
26
27
28
29
30
31
32
33
34
35
36
37
38
39
40
41
42
43
44
45
46
47
48
49
50
51
52
53
54
55
56
57
58
59
60
61
62
63
64
65

376 closely related to the Collodaria, has only been detected in the deep sea (Nakamura et al. in press).
377 Therefore, it is quite possible that unknown Collodaria taxa dominate subsurface layers.
378 Furthermore, some collodarian species are known to exhibit two (or possibly more) morphologies
379 (Biard et al., 2015), and it is possible that they change their distribution depth, depending on life
380 stage. For example, Collodaria increase their colony size *via* asexual reproduction in surface
381 layers and by sexual reproduction in deeper layers. Further studies are needed to clarify the life
382 cycle of radiolarians.

383 The vertical distribution of Gymnodinales and Syndiniales sequence reads showed the
384 opposite trend; the relative abundances of Gymnodinales (and Peridiniales) were smallest at 1000
385 m depth layer, higher closer to the surface, and peaked at surface, whereas, those of Syndiniales
386 sequence reads peaked at 1000 m, lower closer the surface, and lowest at the surface. Many
387 *Karenia* and *Noctiluca* species that cause algal blooms belong to Gymnodinales, which are either
388 autotrophs that perform photosynthesis or heterotrophs that feed on phytoplankton in the euphotic
389 zone of the surface layer (e.g., Gomez, 2007; Guiry and Guiry, 2015; Landsberg et al., 2009).
390 Syndiniales taxa, which parasitize crustaceans, radiolarians, algae, ciliates, and other
391 dinoflagellates, exhibit high diversity and sequence abundance in recent 18S rRNA studies (Bråte
392 et al., 2012; Guillou et al., 2008; van den Hoek et al., 1995; López-García et al., 2001; Strassert
393 et al., 2018). The relatively high abundance of Syndiniales (Alveolata) sequence reads, along with
394 those of radiolarians, at the NPIW suggests that parasitic infections of radiolarians by Syndiniales
395 might play a crucial role in determining the patterns observed in the NPIW ecosystem.

396 It is interesting to note that the relative abundances of Peridiniales sequence reads were
397 highest in the bathypelagic layers (2000–3000 m). Gymnodinales also exhibited relatively high

1
2
3
4
5
6
7
8
9
10
11
12
13
14
15
16
17
18
19
20
21
22
23
24
25
26
27
28
29
30
31
32
33
34
35
36
37
38
39
40
41
42
43
44
45
46
47
48
49
50
51
52
53
54
55
56
57
58
59
60
61
62
63
64
65

398 read numbers in the bathypelagic layers. Syndiniales exhibited relatively high read numbers in
399 the deep layers. Most previous studies of Alveolata have focused on coastal areas or euphotic
400 zones (e.g., Anderson et al., 1998; Gomez, 2007). However, in the present study, Alveolata
401 exhibited consistently large proportions of OTUs and sequence reads, regardless of depth, and
402 accounted for 41–47% of all OTUs and 35–45% of all sequence reads. These results suggest that
403 a few groups of Alveolata (e.g., Peridiniales, Gymnodiniales, and Syndiniales) are abundant in
404 both the surface layer and deeper layers and that such taxa may substantially affect marine
405 ecosystems in relatively shallow coastal areas and euphotic zones, as well as in the entire open
406 ocean ecosystem.

407 Foraminifera are one of the main taxa in the supergroup Rhizaria, which contains more
408 than 4000 species (mostly benthic; Nakamura et al., 2019). However, no Foraminifera sequence
409 reads were detected in the present study, likely because the ribosomal DNA sequences of
410 foraminiferans differ largely from those of other rhizarians (e.g., Radiolaria and Phaeodaria;
411 Ishitani and Takishita, 2015). Radiolaria contain ~1000 described species (excluding extinct
412 species), whereas Cercozoa contain fewer (Nakamura et al., 2015). Radiolarians generally possess
413 solid siliceous skeletons and are larger than cercozoans, which generally have fragile or absent
414 skeletons. Therefore, more radiolarian species have been described, presumably because they are
415 more recognizable microscopically. Considering that the metabarcoding results of the present
416 study indicated similar proportions of Radiolaria and Cercozoa OTUs, previous studies might
417 have underestimated the species diversity of Cercozoa, which are generally parasitic (except for
418 phaeodarians; Nakamura and Suzuki, 2015a).

1
2
3 419 Even though only a single species, *Sticholonche zanclea* Hertwig 1877, is classified in
4
5 420 the Order Taxopodia (Suzuki and Not, 2015), four distinct Taxopodia OTUs were detected in the
6
7
8 421 present study. Thus, some genetically distinct lineages may exist within the Taxopodia. The total
9
10
11 422 read numbers of Taxopodia were generally higher than those of other radiolarian orders and
12
13
14 423 peaked at a depth of 3000 m. These results suggest that Taxopodia taxa are abundant in deep
15
16 424 layers, despite previous reports that they are mainly distributed in the surface and mesopelagic
17
18
19 425 layers (e.g., Suzuki and Not, 2015). Because Taxopodia taxa are genetically and morphologically
20
21
22 426 distinct from other radiolarian orders (Suzuki and Not, 2015), the DNA copy numbers of
23
24 427 Taxopodia taxa might differ from those of other radiolarian orders. It is difficult to ascertain the
25
26
27 428 vertical profile of Phaeodaria OTU numbers since only four OTUs were detected. However, it is
28
29
30 429 worth noting that the OTUs and sequence reads of Phaeodaria were mainly detected in surface
31
32
33 430 layers (50 and 100 m), which corresponds to recent reports that Phaeodaria are occasionally found
34
35
36 431 in shallow layers (Biard and Ohman, 2020). Since several new Phaeodaria species were recently
37
38
39 432 described near the survey area (Nakamura et al., 2013, 2016, 2018), some species might be highly
40
41
42 433 abundant in the surface layers.

43 434

44 435

45 436 **5 Conclusions**

46
47
48 437 The marine ecosystem is greatly affected by physical changes, such as oceanographic structure
49
50
51 438 variation and climate change. Microplankton and primary producers with rapid life cycles are the
52
53
54 439 first to be affected by physical changes and subsequently affect the productivity of meso-
55
56
57 440 macrozooplankton and fishery species located at higher trophic levels. Here, the present study
58
59
60
61
62
63
64
65

1
2
3
4
5
6
7
8
9
10
11
12
13
14
15
16
17
18
19
20
21
22
23
24
25
26
27
28
29
30
31
32
33
34
35
36
37
38
39
40
41
42
43
44
45
46
47
48
49
50
51
52
53
54
55
56
57
58
59
60
61
62
63
64
65

441 demonstrates that the plankton community structure is significantly affected by vertical marine
442 structure in the waters around the Kuroshio Current. In the North Pacific Intermediate Water
443 (NPIW), which is formed in the northwestern Pacific Ocean and extends to the mesopelagic layer
444 around the Kuroshio Current, the diversity of eukaryotic plankton communities is lowest
445 vertically, and the community of the NPIW, isolated from the other vertical layers (surface and
446 bathypelagic), form a unique ecosystem. The Alveolata and Rhizaria communities in the
447 Kuroshio-influenced epipelagic zone exhibited seasonal variation. In oligotrophic waters, such as
448 those around the Kuroshio Current, marine production is especially supported by microplankton.
449 Thus, integrated research on the whole ecosystem, from microplankton to fish species, together
450 with changes in the oceanographic structure, are needed to understand the variation of fishery
451 resources, and to conduct effective fisheries management. In addition, for changes that involve
452 anthropogenic effects, such as climate change and marine resources reduction, it is essential to
453 conduct interdisciplinary research of human societies and natural ecosystems (socio-ecological
454 systems), as well as to implement specific countermeasures based on the findings of such studies.

455
456

457 **Acknowledgements**

458 This work was supported by the Stock Assessment Project, which was commissioned by the
459 Fisheries Agency of Japan and Japan Society for the promotion of Science KAKENHI (grant
460 number JP17J03204). The oceanic observation was supported by the science project "Evaluation,
461 Adaptation and Mitigation of Global Warming in Agriculture, Forestry and Fisheries: Research
462 and Development," which was funded by the Agriculture, Forestry and Fisheries Research

1
2
3
4
5
6
7
8
9
10
11
12
13
14
15
16
17
18
19
20
21
22
23
24
25
26
27
28
29
30
31
32
33
34
35
36
37
38
39
40
41
42
43
44
45
46
47
48
49
50
51
52
53
54
55
56
57
58
59
60
61
62
63
64
65

463 Council of Japan. We are grateful to the captains, crews, and staff of the *R/V Soyo-Maru* for their
464 cooperation during the monitoring cruise. We are also grateful to Dr. Junya Hirai and Dr. Akihiro
465 Tuji, for valuable advice, and to S. Kakehi, who created the Excel macros for density calculation.
466 We would like to thank the two anonymous reviewers whose comments and suggestions helped
467 improve and clarify this manuscript.

468

469 **References**

470 Anderson, D.M., Cembella, A.D., Hallegraeff, G.M., 1998. Physiological Ecology of Harmful
471 Algal Blooms, NATO ASI Series, Series G, Ecological Sciences. Springer-Verlag, Bermuda.
472 Anderson, M.J., Gorley, R.N., Clarke, K.R., 2008. PERMANOVA+ for PRIMER: Guide to
473 Software and Statistical Methods. PRIMER-E, Plymouth.
474 Barkley, R.A., 1970. The Kuroshio current. *Science J.* 6, 54–60. [https://swfsc-](https://swfsc-publications.fisheries.noaa.gov/publications/CR/1973/7302.PDF)
475 [publications.fisheries.noaa.gov/publications/CR/1973/7302.PDF](https://swfsc-publications.fisheries.noaa.gov/publications/CR/1973/7302.PDF)
476 Bescot, N.L., Mahé, F., Audic, S., Dimier, C., Garet, M., Pulain, J., Wincker, P., de Vargas, C.,
477 Siano, R., 2016. Global patterns of pelagic dinoflagellate diversity across protist size classes
478 unveiled by metabarcoding. *Environ. Microbiol.* 18, 609–626. [https://doi.org/10.1111/1462-](https://doi.org/10.1111/1462-2920.13039)
479 [2920.13039](https://doi.org/10.1111/1462-2920.13039)
480 Biard, T., Ohman, M.D., 2020. Vertical niche definition of test-bearing protists (Rhizaria) into
481 the twilight zone revealed by in situ imaging. *Limn. Oceanogr.* 65, 2583–2602.
482 <https://doi.org/10.1101/573410>

1
2
3
4
5
6
7
8
9
10
11
12
13
14
15
16
17
18
19
20
21
22
23
24
25
26
27
28
29
30
31
32
33
34
35
36
37
38
39
40
41
42
43
44
45
46
47
48
49
50
51
52
53
54
55
56
57
58
59
60
61
62
63
64
65

483 Biard, T., Pilleta, L., Decelle, J., Poirier, C., Suzukie, N., Not, F., 2015. Towards an Integrative
484 Morpho-molecular Classification of the Collodaria (Polycystinea, Radiolaria). *ISME J.* 10,
485 945–958. <https://doi.org/10.1038/ismej.2015.170>

486 Biard, T., Stemmann, L., Picheral, M., Mayot, N., Vandromme, P., Hauss, H., Gorsky, G., Guidi,
487 L., Kiko, R., Not, F., 2016. In situ imaging reveals the biomass of giant protists in the global
488 ocean. *Nature*. 532, 504–507. <https://doi.org/10.1038/nature17652>

489 Bråte, J., Krabberød, A.K., Dolven, J.K., Ose, R.F., Kristensen, T., Bjørklund, K.R., Shalchian-
490 Tabrizi, K., 2012. Radiolaria associated with large diversity of marine alveolates. *Protist*. 163,
491 767–777. <https://doi.org/10.1016/j.protis>

492 Brisbin, M.M., Brunner, O.D., Grossmann, M.M., Mitarai, S., 2020. Paired high- throughput, in
493 situ imaging and high- throughput sequencing illuminate acantharian abundance and vertical
494 distribution. *Limnol. Oceanog.* 9999, 1–13. <https://doi.org/10.1002/lno.11567>

495 Camacho, C., Coulouris, G., Avagyan, V., Ma, N., Papadopoulos, J., Bealer, K., Madden, T.L.,
496 2009. BLAST+: architecture and applications. *BMC Bioinform.* 10, 421.
497 <https://doi.org/10.1186/1471-2105-10-421>

498 Canals, O., Obiol, A., Muhovic, I., Vaqué, D., Massana, R., 2020. Ciliate diversity and
499 distribution across horizontal and vertical scales in the open ocean. *Mol. Ecol.* 29, 2824–
500 2839. <https://doi.org/10.1111/mec.15528>

501 Cheung, M., Au, C., Chu, K., Kwan, H., Wong, C., 2010. Composition and genetic diversity of
502 picoeukaryotes in subtropical coastal waters as revealed by 454 pyrosequencing. *ISME J.* 4,
503 1053–1059. <https://doi.org/10.1038/ismej.2010.26>

1
2
3
4
5
6
7
8
9
10
11
12
13
14
15
16
17
18
19
20
21
22
23
24
25
26
27
28
29
30
31
32
33
34
35
36
37
38
39
40
41
42
43
44
45
46
47
48
49
50
51
52
53
54
55
56
57
58
59
60
61
62
63
64
65

504 Clarke, K.R., 1993. Non- parametric multivariate analyses of changes in community
505 structure. *Austral Ecol.* 18, 117–143. [https://doi.org/ 10.1111/j.1442-](https://doi.org/10.1111/j.1442-9993.1993.tb00438.x)
506 [9993.1993.tb00438.x](https://doi.org/10.1111/j.1442-9993.1993.tb00438.x)

507 Clarke, K.R., Gorley, R.N., 2015. *PRIMER v7: User Manual/Tutorial*. PRIMER-E,
508 Plymouth.

509 Countway, P.D., Gast, R.J., Dennett, M.R., Savai, P., Rose, J.M., Caron, D.A., 2007. Distinct
510 protistan assemblages characterize the euphotic zone and deep sea (2500 m) of the western
511 North Atlantic (Sargasso Sea and Gulf Stream): Protistan diversity in the euphotic zone and
512 deep sea. *Environ. Microbiol.* 9, 1219–1232. [https://doi.org/10.1111/j.1462-](https://doi.org/10.1111/j.1462-2920.2007.01243.x)
513 [2920.2007.01243.x](https://doi.org/10.1111/j.1462-2920.2007.01243.x)

514 Edgar, R.C., Haas, B.J., Clemente, J.C., Quince, C., Knight, R., 2011. UCHIME improves
515 sensitivity and speed of chimera detection. *Bioinform.* 27, 2194–2200.
516 <https://doi.org/10.1093/bioinformatics/btr381>

517 Endo, H., Suzuki, K., 2019. Spatial variations in community structure of haptophytes across the
518 Kuroshio front in the Tokara Strait, in: Nagai, T., Saito, H., Suzuki, K., Takahashi, M. (Eds.),
519 Kuroshio Current: Physical, Biogeochemical and Ecosystem Dynamics. AGU Geophysical
520 Monograph Series, AGU-Wiley, pp. 207–221.

521 Gomez, F., 2007. Gymnodinioid Dinoflagellates (Gymnodiniales, Dinophyceae) in the Open
522 Pacific Ocean. *Algae.* 22, 273–286. <https://doi.org/10.4490/algae.2007.22.4.273>

523 Guillou, L., Viprey, M., Chambouvet, A., Welsh, R.M., Kirkham, A.R., Massana, R., Scanlan,
524 D.J., Worden, A.Z., 2008. Widespread occurrence and genetic diversity of marine parasitoids

1
2
3
4
5
6
7
8
9
10
11
12
13
14
15
16
17
18
19
20
21
22
23
24
25
26
27
28
29
30
31
32
33
34
35
36
37
38
39
40
41
42
43
44
45
46
47
48
49
50
51
52
53
54
55
56
57
58
59
60
61
62
63
64
65

525 belonging to *Syndiniales* (*Alveolata*). *Environ. Microbiol.* 10, 3349–3365.
526 <https://doi.org/10.1111/j.1462-2920.2008.01731.x>

527 Guiry, M.D., Guiry, G.M., 2015. *AlgaeBase*. National University of Ireland, Galway.
528 <https://www.algaebase.org>

529 Gutierrez-Rodriguez, A., Stukel, M.R., dos Santos, A.L., Biard, T., Scharek, R., Vaultot, D.,
530 Landry, M.R., Not, F., 2019. High contribution of Rhizaria (Radiolaria) to vertical export in
531 the California Current Ecosystem revealed by DNA metabarcoding. *ISME J.* 13, 964–976.
532 <https://doi.org/10.1038/s41396-018-0322-7>

533 Harris, P.G., Lang, G., 2014. *Routledge handbook of environment and society in Asia*, 1st ed.
534 Routledge, New York.

535 Hirai, J., Katakura, S., Kasai, H., Nagai, S., 2017. Cryptic zooplankton diversity revealed by a
536 metagenetic approach to monitoring metazoan communities in the coastal waters of the
537 Okhotsk Sea, northeastern Hokkaido. *Front. Mar. Sci.* 4, 379.
538 <https://doi.org/10.3389/fmars.2017.00379>

539 Hu, S.K., Campbell, V., Connell, P., Gellene, A.G., Liu, Z., Terrado, R., Caron, D.A., 2016.
540 Protistan diversity and activity inferred from RNA and DNA at a coastal ocean site in the
541 eastern North Pacific. *FEMS Microb. Ecol.* 92, fiw050.
542 <https://doi.org/10.1093/femsec/fiw050>

543 Ichikawa, T., 2008. Analysis of the community structure of meso-zooplankton in the Oyashio and
544 transition zone using video plankton recorder (VPRII). *Bull. Fish. Res. Agen.* 24, 23–104.
545 (abstract in English) <https://www.fra.affrc.go.jp/bulletin/bull/bull24/ichikawa.pdf>

1
2
3
4
5
6
7
8
9
10
11
12
13
14
15
16
17
18
19
20
21
22
23
24
25
26
27
28
29
30
31
32
33
34
35
36
37
38
39
40
41
42
43
44
45
46
47
48
49
50
51
52
53
54
55
56
57
58
59
60
61
62
63
64
65

546 Ichikawa, T., Segawa, K., Terazaki, M., 2007. Estimation of Cnidaria and Ctenophora biomass
547 and vertical distribution using the video plankton recorder II (VPRII) in the meso- and
548 epipelagic layers of the Oyashio and transition zone off eastern Japan. Bull. Jpn. Soc. Fish.
549 Oceanogr. 70, 240–248. (abstract in English)

550 Illumina (2013) 16S metagenomic sequencing library preparation: preparing 16S ribosomal gene
551 amplicons for the Illumina MiSeq system (part no. 15044223 Rev. B).

552 Imasaki, S., Uchida, H., Ichikawa, H., Fukasawa, M., Umatani, S., the ASUKA Group, 2001.
553 Satellite altimeter monitoring the Kuroshio transport south of Japan. Geophys. Res. Lett. 28,
554 17–20. <https://doi.org/10.1029/2000GL011796>

555 Ishitani, Y., Takishita, K., 2015. “Retaria” hypothesis, a sister relationship between Foraminifera
556 and Radiolaria. Fossils. 96, 13–21. (abstract in English) [http://www.palaeo-soc-](http://www.palaeo-soc-japan.jp/publications/9398452d90e9905a714ff81c0c8de031c08cdf4f.pdf)
557 [japan.jp/publications/9398452d90e9905a714ff81c0c8de031c08cdf4f.pdf](http://www.palaeo-soc-japan.jp/publications/9398452d90e9905a714ff81c0c8de031c08cdf4f.pdf)

558 Kanagawa Prefectural Fisheries Technology Center: Flash report on hydrographic conditions of
559 Kanto-Tokai, the adjacent water of the Izu Islands. [http://sui-](http://sui-kanagawa.jp/Kaikyozu/KantoToka iZ)
560 [kanagawa.jp/Kaikyozu/KantoToka iZ](http://sui-kanagawa.jp/Kaikyozu/KantoToka iZ)

561 Kobari, T., Honma, T., Hasegawa, D., Yoshie, N., Tsutsumi, E., Matsuno, T., Nagai, T.,
562 Kanayama, T., Karu, F., Suzuki, K., Tanaka, T., Guo, X., Kume, G., Nishina, A., Nakamura,
563 H., 2020. Phytoplankton growth and consumption by microzooplankton stimulated by
564 turbulent nitrate flux suggest rapid trophic transfer in the oligotrophic Kuroshio.
565 Biogeosciences. 17, 2441–2452. <https://doi.org/10.5194/bg-17-2441-2020>

1
2
3
4
5
6
7
8
9
10
11
12
13
14
15
16
17
18
19
20
21
22
23
24
25
26
27
28
29
30
31
32
33
34
35
36
37
38
39
40
41
42
43
44
45
46
47
48
49
50
51
52
53
54
55
56
57
58
59
60
61
62
63
64
65

566 Kok, S.P., Kikuchi, T., Toda, T., Kurosawa, N., 2012. Diversity and community dynamics of
567 protistan microplankton in Sagami Bay revealed by 18S rRNA gene clone analysis. *Plankton*
568 *Benthos Res.* 7, 75–86.

569 Kuroda, H., Takasuka, A., Hirota, Y., Kodama, T., Ichikawa, T., Takahashi, D., Aoki, K., Setou,
570 T. 2018. Numerical experiments based on a coupled physical–biochemical ocean model to
571 study the Kuroshio-induced nutrient supply on the shelf-slope region off the southwestern
572 coast of Japan. *J. Mar. Syst.* 179, 38–54

573 Landsberg, J.H., Flewelling, L.J., Naar, J., 2009. *Karenia brevis* red tides, brevetoxins in the food
574 web, and impacts on natural resources: Decadal advancements. *Harmful Algae.* 8, 598–607,
575 doi:10.1016/j.hal.2008.11.010

576 Li, W., Godzik, A., 2006. Cd-hit: a fast program for clustering and comparing large sets of protein
577 or nucleotide sequences. *Bioinform.* 22, 1658–1659.
578 <https://doi.org/10.1093/bioinformatics/btl158>

579 Lindeque, P.K., Parry, H.E., Harmer, R.A., Somerfield, P.J., Atkinson, A., 2013. Next Generation
580 Sequencing Reveals the Hidden Diversity of Zooplankton Assemblages. *PLoS ONE.* 8,
581 e81327. <https://doi.org/10.1371/journal.pone.0081327>

582 López-García, P., Rodríguez-Valera, F., Pedrós-Alió, C., Moreira, D., 2001. Unexpected diversity
583 of small eukaryotes in deep-sea Antarctic plankton. *Nature.* 409, 603–607

584 Masujima, M., Yasuda, I., Hiroe, Y., Watanabe, T., 2003. Transport of Oyashio water across the
585 subarctic front into the mixed water region and formation of NPIW. *J. Oceanogr.* 59, 855–
586 869. <https://doi.org/10.1023/B:JOCE.0000009576.09079.f5>

1
2
3
4
5
6
7
8
9
10
11
12
13
14
15
16
17
18
19
20
21
22
23
24
25
26
27
28
29
30
31
32
33
34
35
36
37
38
39
40
41
42
43
44
45
46
47
48
49
50
51
52
53
54
55
56
57
58
59
60
61
62
63
64
65

587 Matsumoto, Y.T., Yamaguchi, A., 2020. Seasonal changes in the community structure of
588 chaetognaths and the life cycle of the dominant chaetognath *Eukrohnia hamata* in the
589 Oyashio region, western subarctic Pacific. *Plankton Benthos Res.* 15, 146–155.
590 <https://doi.org/10.3800/pbr.15.146>

591 Miyazawa, Y., Zhang, R., Guo, X., Tamura, H., Ambe, D., Lee, J.S., Okuno, A., Yoshinari, H.,
592 Setou, T., Komatsu, K., 2009. Water Mass Variability in the Western North Pacific Detected
593 in a 15-Year Eddy Resolving Ocean Reanalysis. *J. Oceanogr.* 65, 737–756.

594 Mohrbeck, I., Raupach, M.J., Arbizu, P.M., Kneibelsberger, T., Laakmann, S., 2015. High-
595 throughput sequencing—the key to rapid biodiversity assessment of marine Metazoa. *PLoS*
596 *ONE.* 10, e0140342. <https://doi.org/10.1371/journal.pone.0140342>

597 Morimoto, H., 2010. Temporal and spatial changes in the reproductive characteristics of female
598 Japanese sardine *Sardinops melanostictus* and their effects on population dynamics. *Bull. Jpn.*
599 *Soc. Fish. Oceanogr.* 74, 35–45. (in Japanese with English abstract).

600 Morita, H., Toyokawa, M., Hidaka, K., Nishimoto, A., Sugisaki, H., Kikuchi, T., 2017. Spatio-
601 temporal structure of the jellyfish community in the transition zone of cold and warm currents
602 in the northwest Pacific. *Plankton Benthos Res.* 12, 266–284.

603 Nagai, S., Yamamoto, K., Hata, N., Itakura, S., 2012. Study of DNA extraction methods for use
604 in loop-mediated isothermal amplification detection of single resting cysts in the toxic
605 dinoflagellates *Alexandrium tamarense* and *A. catenella*. *Mar. Genom.* 7, 51–56.
606 <https://doi.org/10.1016/j.margen.2012.03.002>.

1
2
3
4
5
6
7
8
9
10
11
12
13
14
15
16
17
18
19
20
21
22
23
24
25
26
27
28
29
30
31
32
33
34
35
36
37
38
39
40
41
42
43
44
45
46
47
48
49
50
51
52
53
54
55
56
57
58
59
60
61
62
63
64
65

607 Nagai, T., Saito, H., Suzuki, K., Takahashi, M., 2019. Kuroshio current: physical, biogeochemical,
608 and ecosystem dynamics (Geophysical Monograph Series) 1st ed. American Geophysical
609 Union, Hoboken.

610 Nakamura, Y., Suzuki, N., 2015a. Biology of widely distributed marine protists, Phaeodaria
611 (Rhizaria, Cercozoa). Bull. Plankton Soc. Japan. 62,110–122. (in Japanese with English
612 abstract)

613 Nakamura, Y., Imai, I., Yamaguchi, A., Tuji, A., Suzuki, N., 2013. *Aulographis japonica* sp. nov.
614 (Phaeodaria, Aulacanthida, Aulacanthidae), an abundant zooplankton in the deep sea of the
615 Sea of Japan. Plankton Benthos Res. 8, 107–115.

616 Nakamura, Y., Imai, I., Yamaguchi, A., Tuji, A., Not, F., Suzuki, N., 2015. Molecular phylogeny
617 of the widely distributed marine protists Phaeodaria (Rhizaria, Cercozoa). Protist. 166, 363–
618 373. <https://doi.org/10.1016/j.protis.2015.05.004>

619 Nakamura, Y., Imai, I., Tuji, A., Suzuki, N., 2016. A new phaeodarian species discovered from
620 the Japan Sea Proper Water, *Aulosцена pleuroclada* sp. nov. (Aulosphaeridae,
621 Phaeosphaerida, Phaeodaria). J. Eukaryot. Microbiol. 63, 271–274.
622 <https://doi.org/10.1111/jeu.12274>

623 Nakamura, Y., Somiya, R., Kanda, M., Yamaguchi, A., Tuji, A., Hori, R.S., 2018. *Gazelletta*
624 *kashiwaensis* sp. nov. (Medusettidae, Phaeodaria, Cercozoa), Its Morphology, Phylogeny,
625 Distribution and Feeding Behavior. J. Eukaryot. Microbiol. 65, 923–927
626 <https://doi.org/10.1111/jeu.12516>.

627 Nakamura, Y., Matsuoka, K., Imai, I., Ishii, K., Kuwata, A., Kawachi, M., Kimoto, K., Suzuki,
628 N., Sano, M., Landeira, J.M., Miyamoto, H., Nishioka, J., Nishida, S., 2019. Updated

1
2
3
4
5
6
7
8
9
10
11
12
13
14
15
16
17
18
19
20
21
22
23
24
25
26
27
28
29
30
31
32
33
34
35
36
37
38
39
40
41
42
43
44
45
46
47
48
49
50
51
52
53
54
55
56
57
58
59
60
61
62
63
64
65

629 information on plankton groups — the current status of the taxonomy and ecology. Bull.
630 Plankton Soc. Japan. 66, 22–40. (in Japanese with English abstract)

631 Nakamura, Y., Tuji, A., Kimoto, K., Yamaguchi, A., Hori, R.S., Suzuki, N., Ecology, morphology,
632 phylogeny and taxonomic revision of giant radiolarians, *Orodaria* ord. nov. (Radiolaria;
633 Rhizaria; SAR). Protist. 172, 125808. <https://doi.org/10.1016/j.protis.2021.125808>

634 Not, F., Gausling, R., Azam, F., Heidelberg, J.F., Worden, A.Z., 2007. Vertical distribution of
635 picoeukaryotic diversity in the Sargasso Sea. Env. microbiol. 9, 1233–1252.
636 <https://doi.org/10.1111/j.1462-2920.2007.01247.x>

637 Ohtsuka, S., Nishida, S., 2017. Copepod biodiversity in Japan: Recent advances in Japanese
638 copepodology (Chapter 22), in Motokawa, M., Kajihara, H. (Eds.), Species diversity of
639 animals in Japan, diversity and commonality in animals. Springer, Japan, pp. 565–602.
640 https://doi.org/10.1007/978-4-431-56432-4_22

641 Ollison, G.A., Hu, S.K., Mesrop, Y., DeLong, E.F., Caron, D.A., 2021. Come rain or shine: Depth
642 not season shapes the active protistan community at station ALOHA in the North Pacific
643 Subtropical Gyre. Deep Sea Res. Part I. Oceanogr. Res. Pap. 170, 103494.
644 <https://doi.org/10.1016/j.dsr.2021.103494>

645 Ortiz, J.D., Mix, A.C., Rugh, W., Watkins, J.M., Collier, R.W., 1996. Deep-dwelling planktonic
646 foraminifera of the northeastern Pacific Ocean reveal environmental control of oxygen and
647 carbon isotopic disequilibrium. Geochim. Cosmochim. Acta. 60, 4509–4523.
648 [https://doi.org/10.1016/S0016-7037\(96\)00256-6](https://doi.org/10.1016/S0016-7037(96)00256-6)

1
2
3
4
5
6
7
8
9
10
11
12
13
14
15
16
17
18
19
20
21
22
23
24
25
26
27
28
29
30
31
32
33
34
35
36
37
38
39
40
41
42
43
44
45
46
47
48
49
50
51
52
53
54
55
56
57
58
59
60
61
62
63
64
65

649 Pernice, M.C., Giner, C.R., Logares, R., Perera-Bel, J., Acinas, S.G., Duarte, C.M., Gasol, J.M.,
650 Massana, R., 2016. Large variability of bathypelagic microbial eukaryotic communities.
651 ISME J. 10, 945–958. <https://doi.org/10.1038/ismej.2015.170>

652 Pielou, E.C., 1966. The measurement of diversity in different types of biological collections. J.
653 Theor. Biol. 13, 131–144. [https://doi.org/10.1016/0022-5193\(66\)90013-0](https://doi.org/10.1016/0022-5193(66)90013-0)

654 Preston, C.M., Durkinb, C.A., Yamahara, K.M., 2019. DNA metabarcoding reveals organisms
655 contributing to particulate matter flux to abyssal depths in the North East Pacific Ocean. Deep
656 Sea Res. Part II. 173, 104708. <https://doi.org/10.1016/j.dsr2.2019.104708>

657 Qiu, B., Lukas, R., 1996. Seasonal and interannual variability of the North Equatorial Current,
658 the Mindanao Current, and the Kuroshio along the Pacific western boundary. J. Geophys.
659 Res. 10, 12315–12330. <https://doi.org/10.1029/95JC03204>

660 Reid, J.L. Jr., 1965. Intermediate waters of the Pacific Ocean. The Johns Hopkins Oceanographic
661 Studies.

662 Ruppert, K.M., Kline, R.J., Rahman, M.S., 2019. Past, present, and future perspectives of
663 environmental DNA (eDNA) metabarcoding: A systematic review in methods, monitoring,
664 and applications of global eDNA. Global Ecol. Cons. 17, e00547.
665 <https://doi.org/10.1016/j.gecco.2019.e00547>

666 Sassa, C., Tsukamoto, Y., Nishiuchi, K., Konishi, Y., 2008. Spawning ground and larval transport
667 processes of jack mackerel *Trachurus japonicus* in the shelf-break region of the southern
668 East China Sea. Shelf. Res. 28, 2574–2583. <https://doi.org/10.1016/j.csr.2008.08.002>

1
2
3
4
5
6
7
8
9
10
11
12
13
14
15
16
17
18
19
20
21
22
23
24
25
26
27
28
29
30
31
32
33
34
35
36
37
38
39
40
41
42
43
44
45
46
47
48
49
50
51
52
53
54
55
56
57
58
59
60
61
62
63
64
65

669 Schloss, P.D., Gevers, D., Westcott, S.L., 2011. Reducing the effects of PCR amplification and
670 sequencing artifacts on 16S rRNA-based studies. PLoS ONE. 6, e27310.
671 <https://doi.org/10.1371/journal.pone.0027310>

672 Shannon, C.E., Weaver, W., 1949. The mathematical theory of communication. University of
673 Illinois Press, Urbana.

674 Schnetzer, A., Moorthi, S.D., Countway, P.D., Gast, R.J., Gilg, I.C., Caron, D.A., 2011. Depth
675 matters: Microbial eukaryote diversity and community structure in the eastern North Pacific
676 revealed through environmental gene libraries. Deep Sea Res. Part I. Oceanogr. Res. Pap. 58,
677 16–26. <https://doi.org/10.1016/j.dsr.2010.10.003>

678 Shimizu, Y., Iwao, T., Yasuda, I., Ito, S., Watanabe, T., Uehara, K., Shikama, N., Nakano, T.,
679 2004. Formation process of North Pacific intermediate water revealed by profiling floats set
680 to drift on 26.7 $\sigma\theta$ isopycnal surface. J. Oceanogr. 60, 453–462.
681 <https://doi.org/10.1023/B:JOCE.0000038061.55914.eb>

682 Sildever, S., Kawakami, Y., Kanno, N., Kasai, H., Shiimoto, A., Katakura, S., Nagai, S., 2019.
683 Toxic HAB species from the Sea of Okhotsk detected by a metagenetic approach, seasonality,
684 and environmental drivers. Harmful Algae. 87, 101631.
685 <https://doi.org/10.1016/j.hal.2019.101631>

686 Sogawa, S., Sugisaki, H., Saito, H., Okazaki, Y., Shimode, S., Kikuchi, T., 2013. Congruence
687 between euphausiid community and water region in the northwestern Pacific: particularly in
688 the Oyashio–Kuroshio Mixed Water Region. J. Oceanogr. 69, 71–85.
689 <https://doi.org/10.1007/s10872-012-0158-0>

1
2
3
4
5
6
7
8
9
10
11
12
13
14
15
16
17
18
19
20
21
22
23
24
25
26
27
28
29
30
31
32
33
34
35
36
37
38
39
40
41
42
43
44
45
46
47
48
49
50
51
52
53
54
55
56
57
58
59
60
61
62
63
64
65

690 Strassert, J.F., Karnkowska, A., Hehenberger, E., Del Campo, J., Kolisko, M., Okamoto, N., Burki,
691 F., Janouškovec, J., Poirier, C., Leonard, G., Hallam, S.J., Richards, T.A., Worden, A.Z.,
692 Santoro, A.E., Keeling, P.J., 2018. Single cell genomics of uncultured marine alveolates
693 shows paraphyly of basal dinoflagellates. *ISME J.* 12, 304–308.
694 <https://doi.org/10.1038/ismej.2017.167>
695 Sugisaki, H., Nonaka, M., Ishizaki, S., Hidaka, K., Kameda, T., Hirota, Y., Takasuka, A., 2010.
696 Status and trends of the Kuroshio region 2003–2008, in: McKinnell, S.M., Dagg, M.J. (Eds.),
697 Marine ecosystems of the North Pacific Ocean 2003–2008. PICES Special Publication 4, pp.
698 330–359.
699 Suter, L., Polanowski, A.M., Clarke, L.J., Kitchener, J.A., Deagle, B.E., 2020. Capturing open
700 ocean biodiversity: Comparing environmental DNA metabarcoding to the continuous
701 plankton recorder. *Mol. Ecol.* 30, 3140–3157. <https://doi.org/10.1111/mec.15587>
702 Suzuki, N., Not, F., 2015. Chapter 8. Biology and Ecology of Radiolaria, in: Ohtsuka, S., Suzuki,
703 T., Horiguchi, T., Suzuki, N., Not, F. (Eds.), *Marine Protists Diversity and Dynamics*.
704 Springer, Tokyo, pp. 179–222.
705 Sverdrup, H., Johnson, M.W., Fleming, R.H., 1942. *The oceans, their physics, chemistry, and*
706 *general biology*. Prentice-Hall, New York.
707 Talley, L.D., 1993. Distribution and Formation of North Pacific Intermediate Water. *J. Phys.*
708 *Oceanogr.* 23: 517–538. <https://doi.org/10.1175/1520->
709 [0485\(1993\)023<0517:DAFONP>2.0.CO;2](https://doi.org/10.1175/1520-0485(1993)023<0517:DAFONP>2.0.CO;2)

1
2
3
4
5
6
7
8
9
10
11
12
13
14
15
16
17
18
19
20
21
22
23
24
25
26
27
28
29
30
31
32
33
34
35
36
37
38
39
40
41
42
43
44
45
46
47
48
49
50
51
52
53
54
55
56
57
58
59
60
61
62
63
64
65

710 Talley, L.D., Nagata, Y., Fujimura, M., Kono, T., Inagake, D., Hirai, M., Okuda, K., 1995. North
711 Pacific intermediate water in the Kuroshio/Oyashio mixed water region. *J. Phys. Oceanogr.*
712 25, 475–501. [https://doi.org/10.1175/1520-0485\(1995\)025<0475:npiwit>2.0.co;2](https://doi.org/10.1175/1520-0485(1995)025<0475:npiwit>2.0.co;2)

713 Tanabe, A.S., Nagai, S., Hida, K., Yasuike, M., Fujiwara, A., Nakamura, Y., Takano, Y.,
714 Katakura, S., 2016. Comparative study of the validity of three regions of the 18S-rRNA gene
715 for massively parallel sequencing-based monitoring of the planktonic eukaryote community.
716 *Mol. Ecol. Resour.* 16: 402–414. <https://doi.org/10.1111/1755-0998.12459>

717 Valentini, A., Taberlet, P., Miaud, C., Civade, R., Herder, J., Thomsen, P.F., Bellemain, E.,
718 Besnard, A., Coissac, E., Boyer, F., Gaboriaud, C., Jean, P., Poulet, N., Roset, N., Copp, G.H.,
719 Geniez, P., Pont, D., Argillier, C., Baudoin, J.M., Peroux, T., Crivelli, A.J., Olivier, A.,
720 Acqueberge, M., Brun, M.L., Møller, P.R., Willerslev, E., Dejean, T., 2015. Next-generation
721 monitoring of aquatic biodiversity using environmental DNA metabarcoding. *Mol. Ecol.* 25,
722 929–942. <https://doi.org/10.1111/mec.13428>

723 Hoek C., Hoek, C. van den, Mann, D., Jahns, H.M., Jahns M., 1995. *Algae: An Introduction to*
724 *Phycology*. Cambridge University Press, New York.

725 Watanabe, Y.W., Harada, K., Ishikawa, K., 1995. Dilution of North Pacific Intermediate Water
726 Studied with Chlorofluorocarbons. *J. Oceanogr.* 51, 133–144.
727 <https://doi.org/10.1007/BF02236521>

728 Wu, P., Li, D., Kong, L., Li, Y., Zhang, H., Xie, Z., Lin, L., Wang, D., 2020. The diversity and
729 biogeography of microeukaryotes in the euphotic zone of the northwestern Pacific Ocean.
730 *Sci. Total Environ.* 698, 134289. <https://doi.org/10.1016/j.scitotenv.2019.134289>

1
2
3
4
5
6
7
8
9
10
11
12
13
14
15
16
17
18
19
20
21
22
23
24
25
26
27
28
29
30
31
32
33
34
35
36
37
38
39
40
41
42
43
44
45
46
47
48
49
50
51
52
53
54
55
56
57
58
59
60
61
62
63
64
65

731 Yamazaki, A., Watanabe, T., Tsunogai, U., Iwase, F., Yamano, H., 2016. A 150-year variation of
732 the Kuroshio transport inferred from coral nitrogen isotope signature. *Paleoceanography*. 31,
733 838–846. <https://doi.org/10.1002/2015PA002880>

734 Yasuda, I., 1997. The origin of the North Pacific intermediate water. *J. Geophys. Res. Oceans*.
735 102, 893–909. <https://doi.org/10.1029/96JC02938>

736 Yasuda, I., 2003. Hydrographic Structure and Variability in the Kuroshio-Oyashio Transition
737 Area. *J. Oceanogr.* 59, 389–402.

738

1
2
3
4
5
6
7
8
9
10
11
12
13
14
15
16
17
18
19
20
21
22
23
24
25
26
27
28
29
30
31
32
33
34
35
36
37
38
39
40
41
42
43
44
45
46
47
48
49
50
51
52
53
54
55
56
57
58
59
60
61
62
63
64
65

739 **Figure captions**

740 **Figure 1.** Survey area and locations of sampling stations in the western North Pacific. Dotted
741 lines indicate the Kuroshio Current axis of each cruise.

742 **Figure 2.** Vertical profiles of the physical and chemical environmental variables in the survey
743 area. The sampling sites were categorized as northern (north of the Kuroshio Current), middle
744 (near the Kuroshio Current axis), or southern (south of the Kuroshio Current).

745 **Figure 3.** Taxonomic compositions of operational taxonomic units (OTUs) and sequence reads
746 detected by 18S rRNA gene metabarcoding using high-throughput sequencing.

747 **Figure 4.** Non-metric, multi-dimensional scaling ordination of oceanic plankton communities.
748 Each plot represents samples collected at a specific depth. Bray-Curtis similarity among the
749 samples was calculated from log-transformed sequence abundance data.

750 **Figure 5.** Diversity of oceanic plankton communities detected by metagenetic analysis with
751 respect to depth.

752 **Figure 6.** Vertical distribution of the eukaryotic plankton community. **(a)** Mean number of
753 operational taxonomic units (OTUs) detected in each depth layer. The upper axis and bar graph
754 represent OTUs of all eukaryotic plankton communities, and the lower axis and line plots
755 represent OTUs of each taxon. **(b)** Distribution of oceanic plankton communities among different
756 depths.

757 **Figure 7.** Taxonomic compositions of Alveolata operational taxonomic units (OTUs) and related
758 sequences detected by 18S rRNA gene metabarcoding using high-throughput sequencing.

759 **Figure 8.** Taxonomic compositions of Rhizaria operational taxonomic units (OTUs) and related
760 sequences detected by 18S rRNA gene metabarcoding using high-throughput sequencing.

1
2
3
4
5
6
7
8
9
10
11
12
13
14
15
16
17
18
19
20
21
22
23
24
25
26
27
28
29
30
31
32
33
34
35
36
37
38
39
40
41
42
43
44
45
46
47
48
49
50
51
52
53
54
55
56
57
58
59
60
61
62
63
64
65

761 **Figure 9.** Cluster dendrogram of Alveolata and Rhizaria. Bray-Curtis similarity among the
762 samples was calculated using log-transformed sequence abundance data.

763 **Figure 10.** Distance-based redundancy analysis (dbRDA) ordination of Alveolata and Rhizaria
764 communities. Each plot represents the samples collected from a specific depth. Bray-Curtis
765 similarity among the samples was calculated using log-transformed sequence abundance data.
766 The dbRDA was constrained by best-fit explanatory variables from a distance-based multivariate
767 linear model (DistLM). In the dbRDA ordination, axes indicate percentage variation, in terms of
768 total community structure, and vector overlays indicate the strength and direction of relationships
769 between individual variables and axes.

770

771 **Figure S1.** Vertical profiles of the chemical environmental variables in the survey area.

772 **Figure S2.** Numbers of operational taxonomic units (OTUs) in Alveolata communities at
773 different depths.

774 **Figure S3.** Relative abundance of Alveolata community sequences at different depths.

775 **Figure S4.** Numbers of operational taxonomic units (OTUs) in Rhizaria communities at different
776 depths.

777 **Figure S5.** Relative abundance of Rhizaria community sequences at different depths.

778

Figure 1

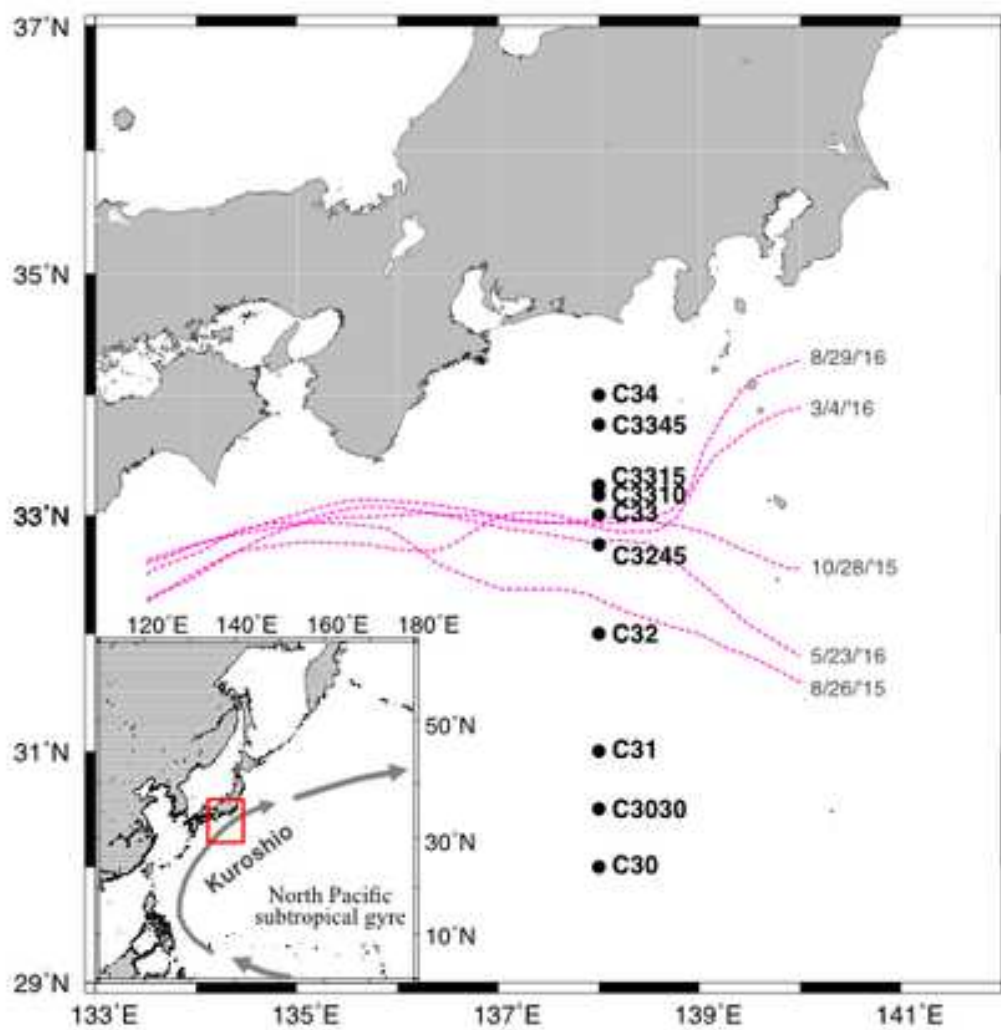


Figure 2

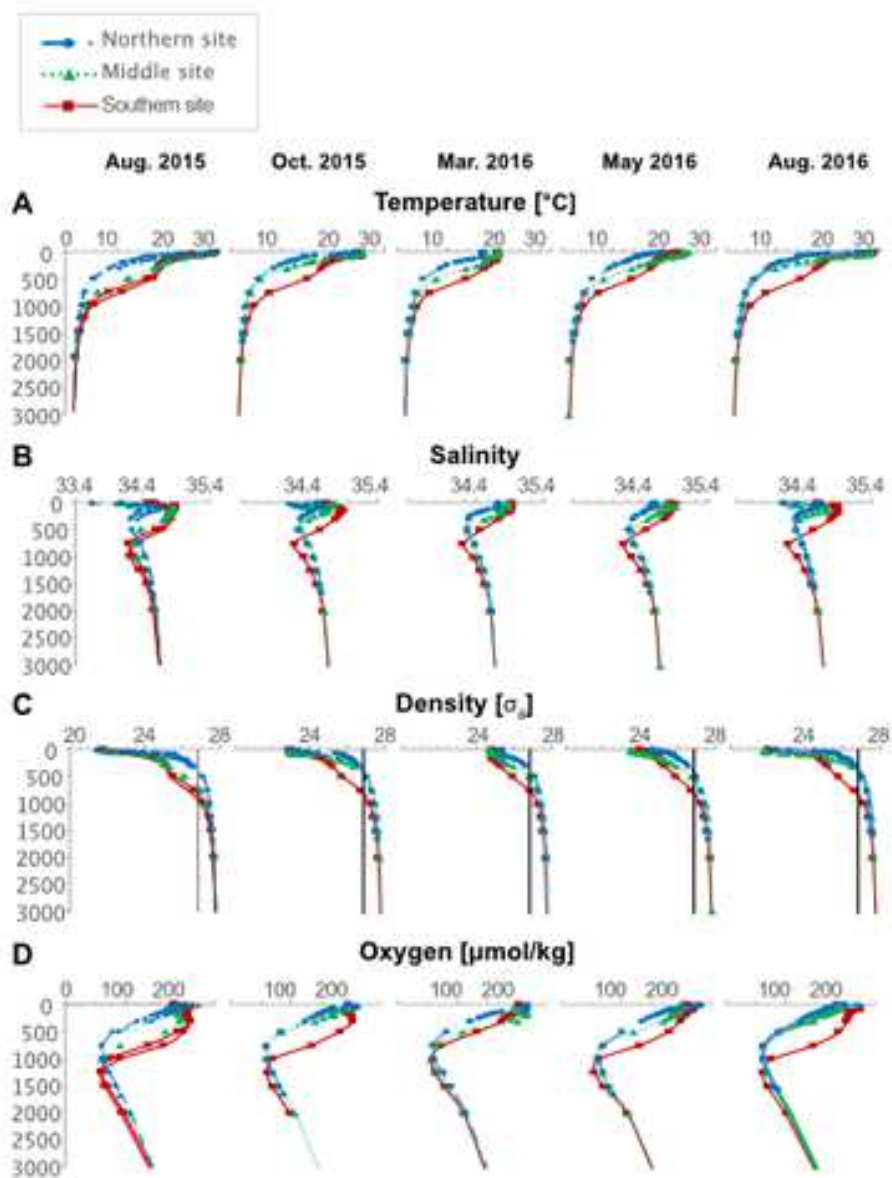


Figure 3

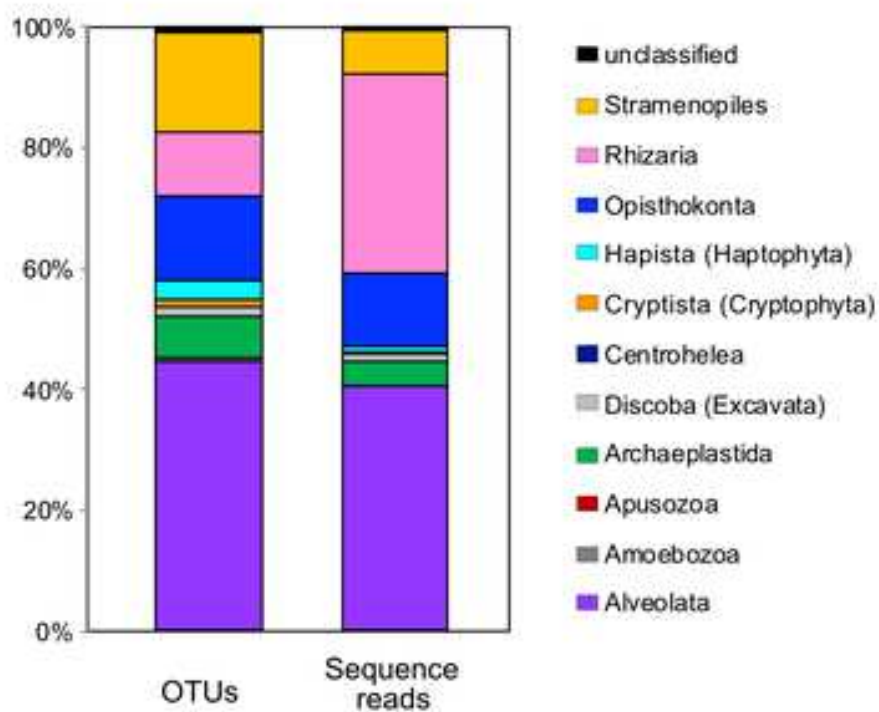


Figure 4

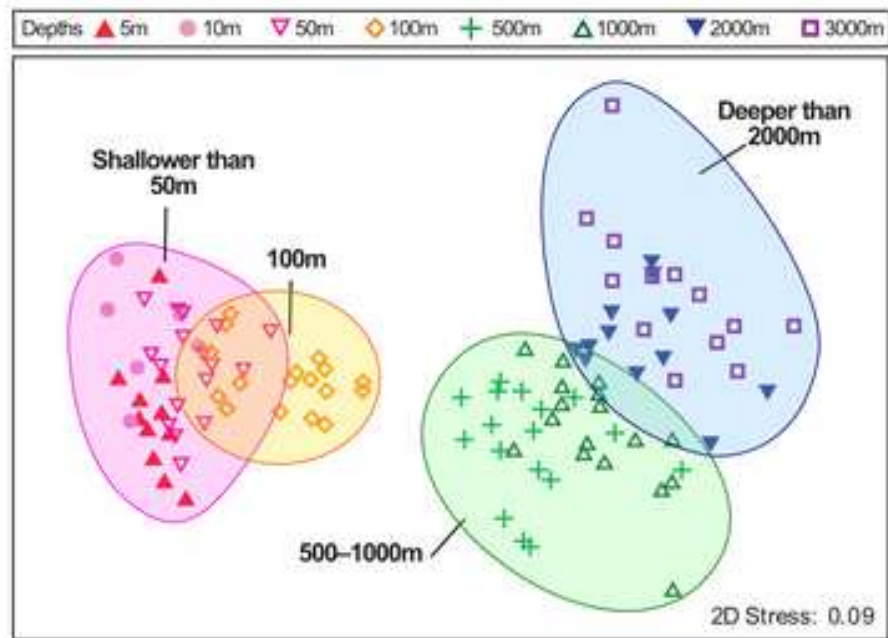


Figure 5

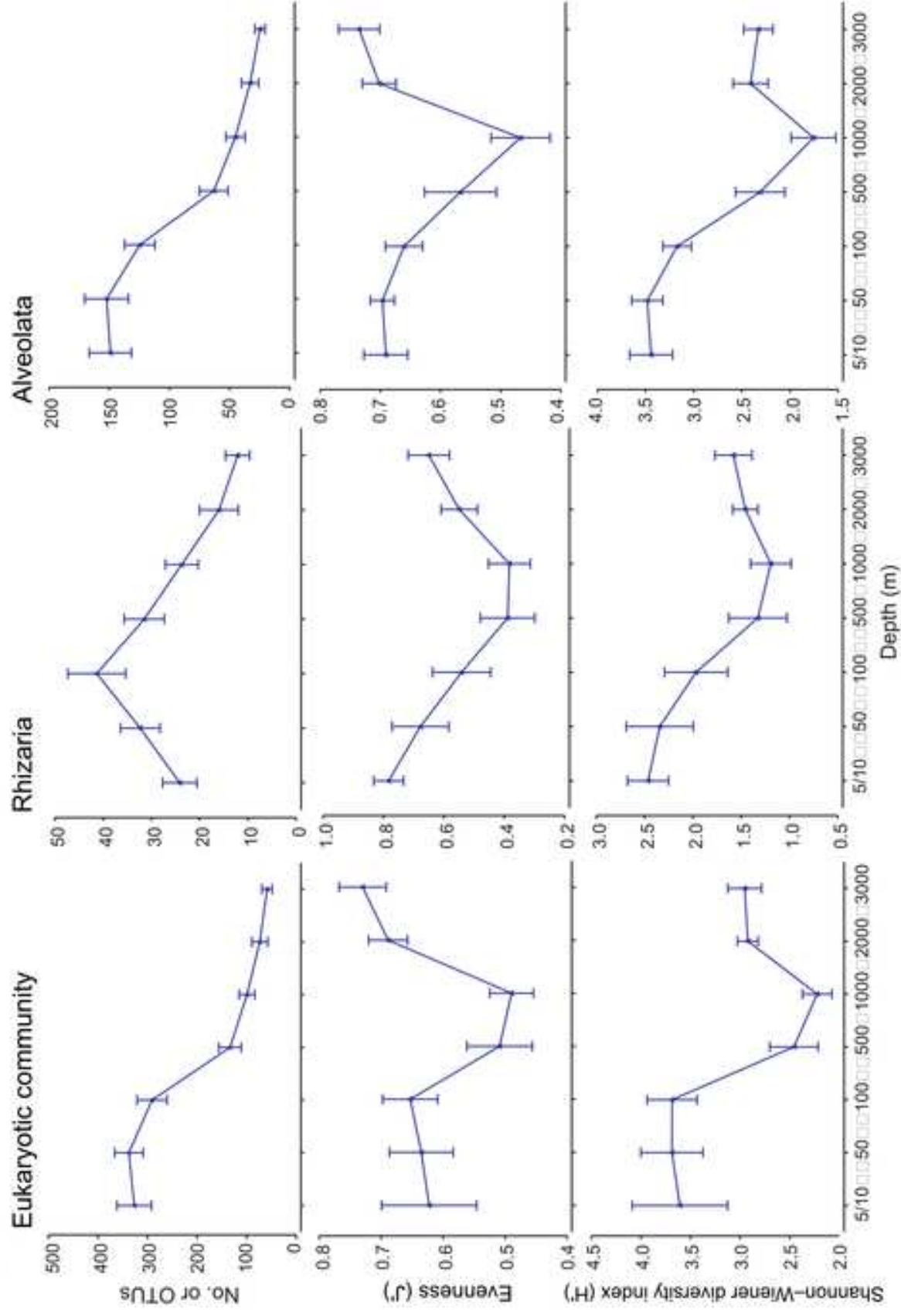


Figure 6

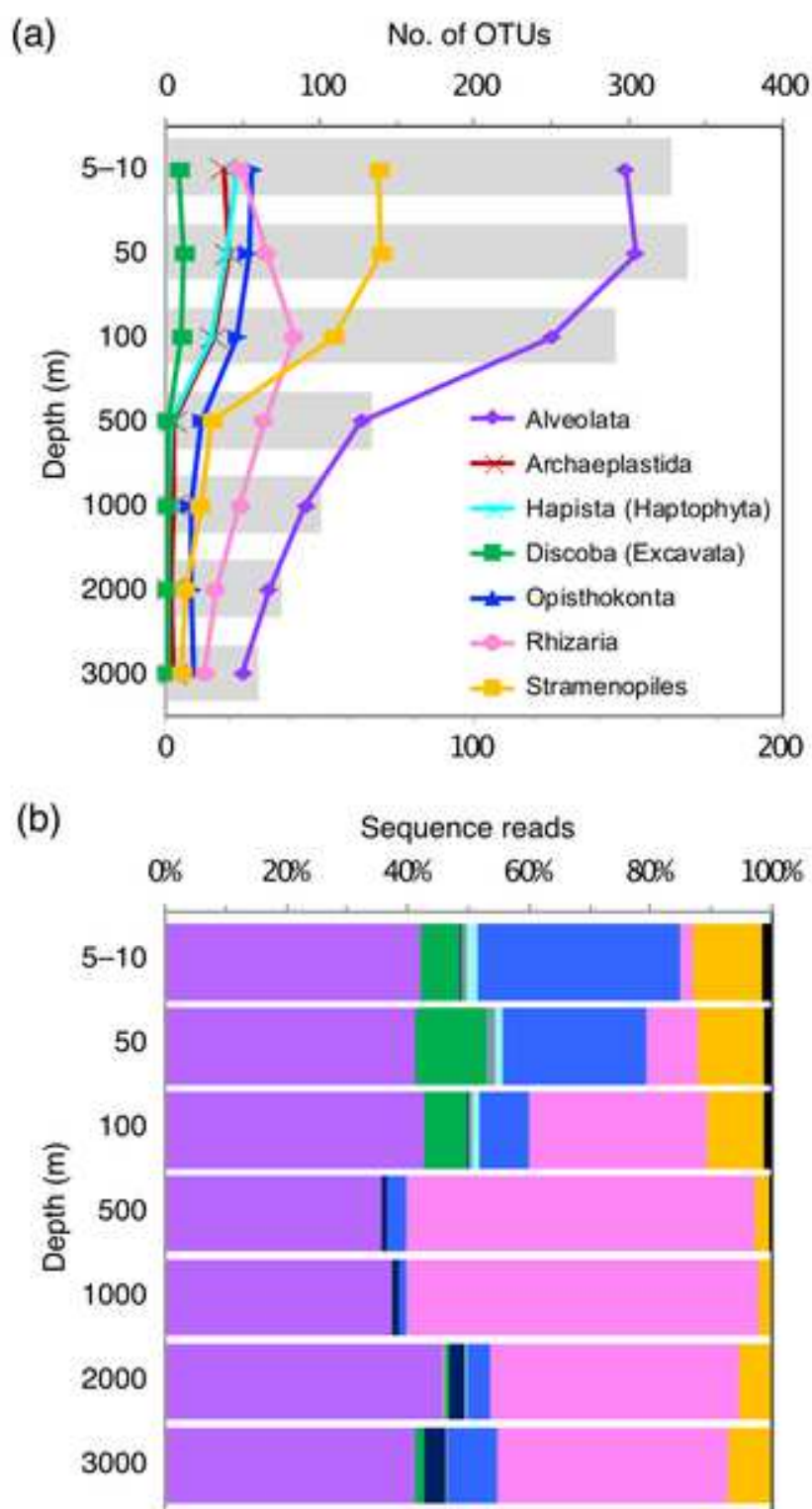


Figure 7

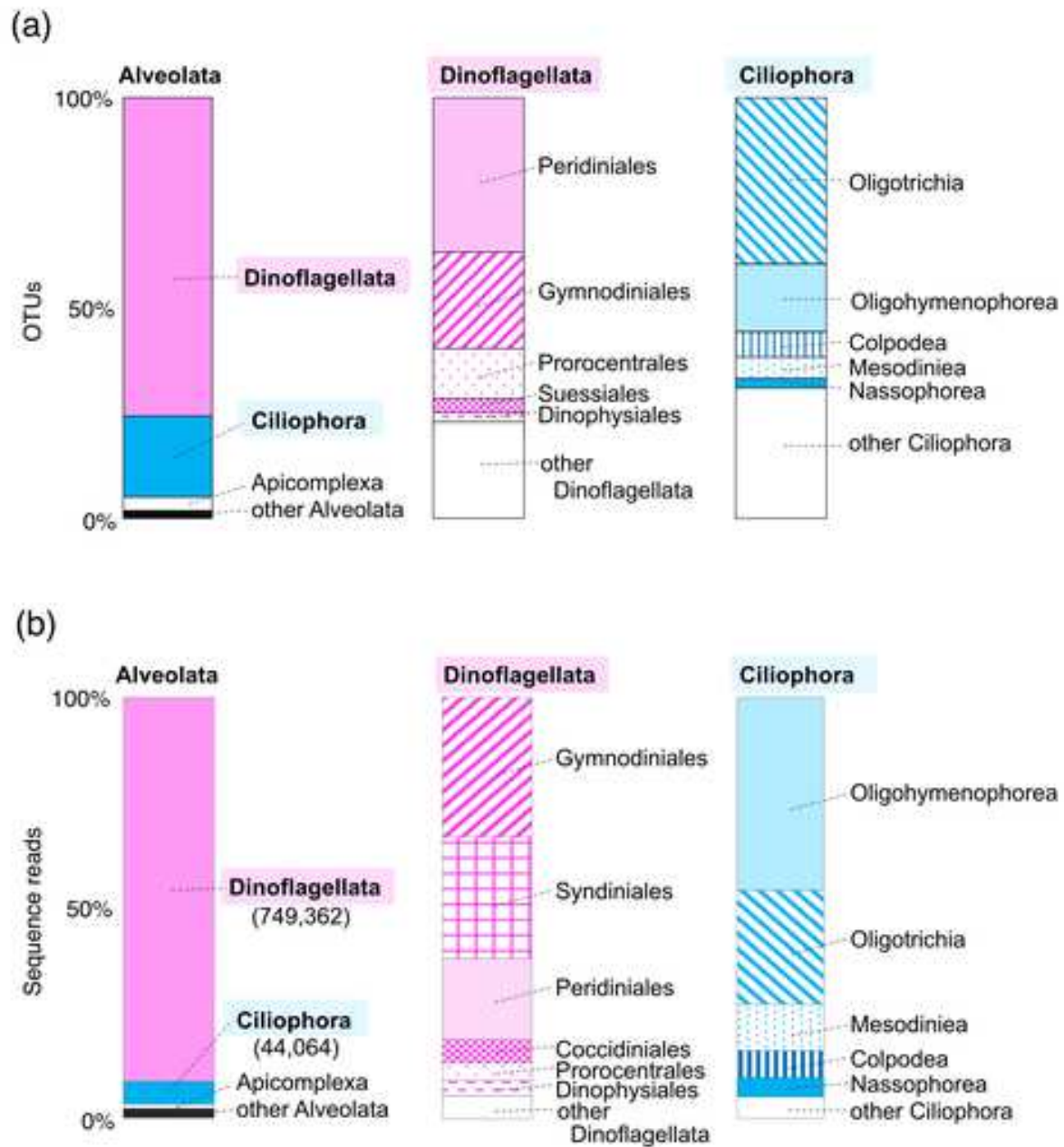


Figure 8

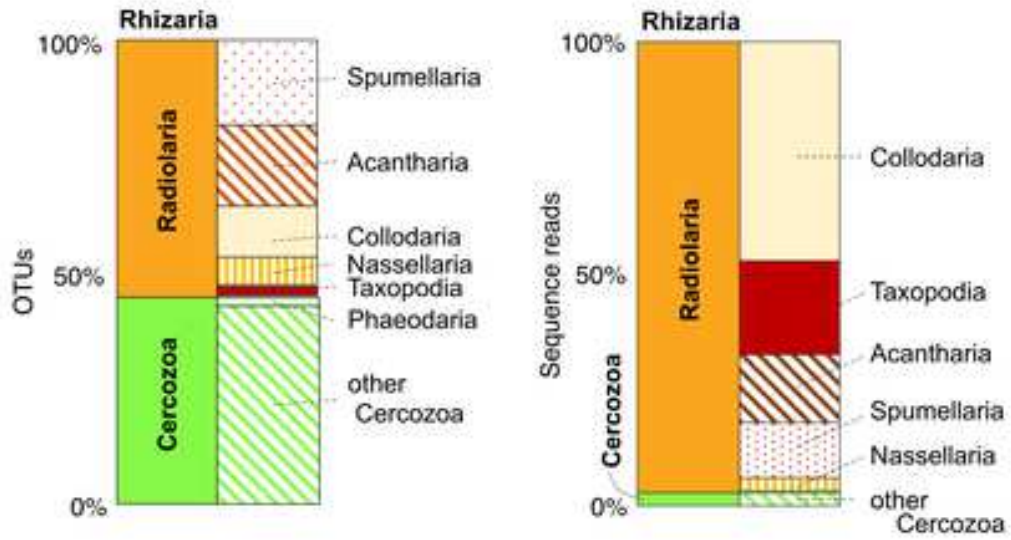


Figure 9

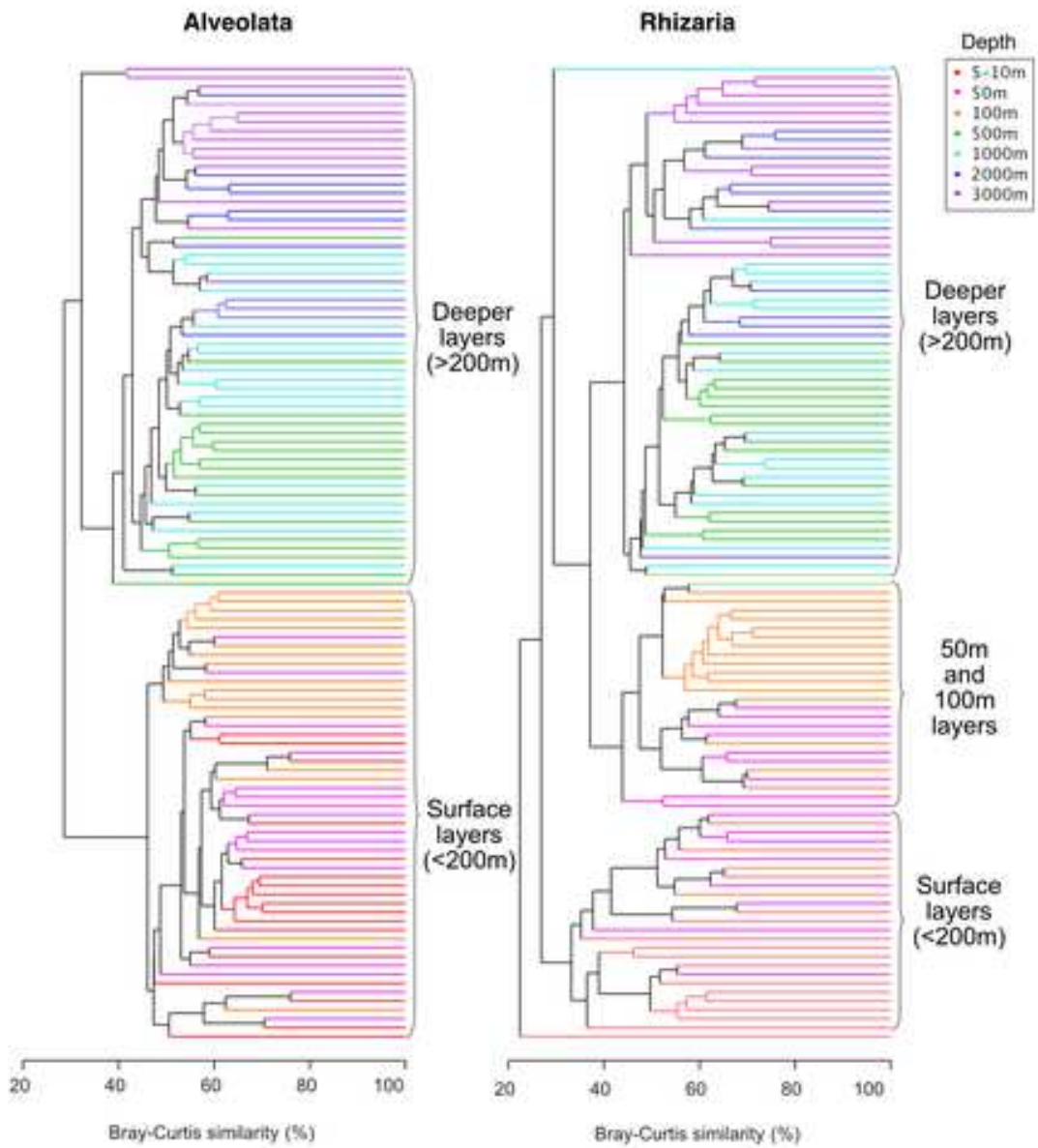
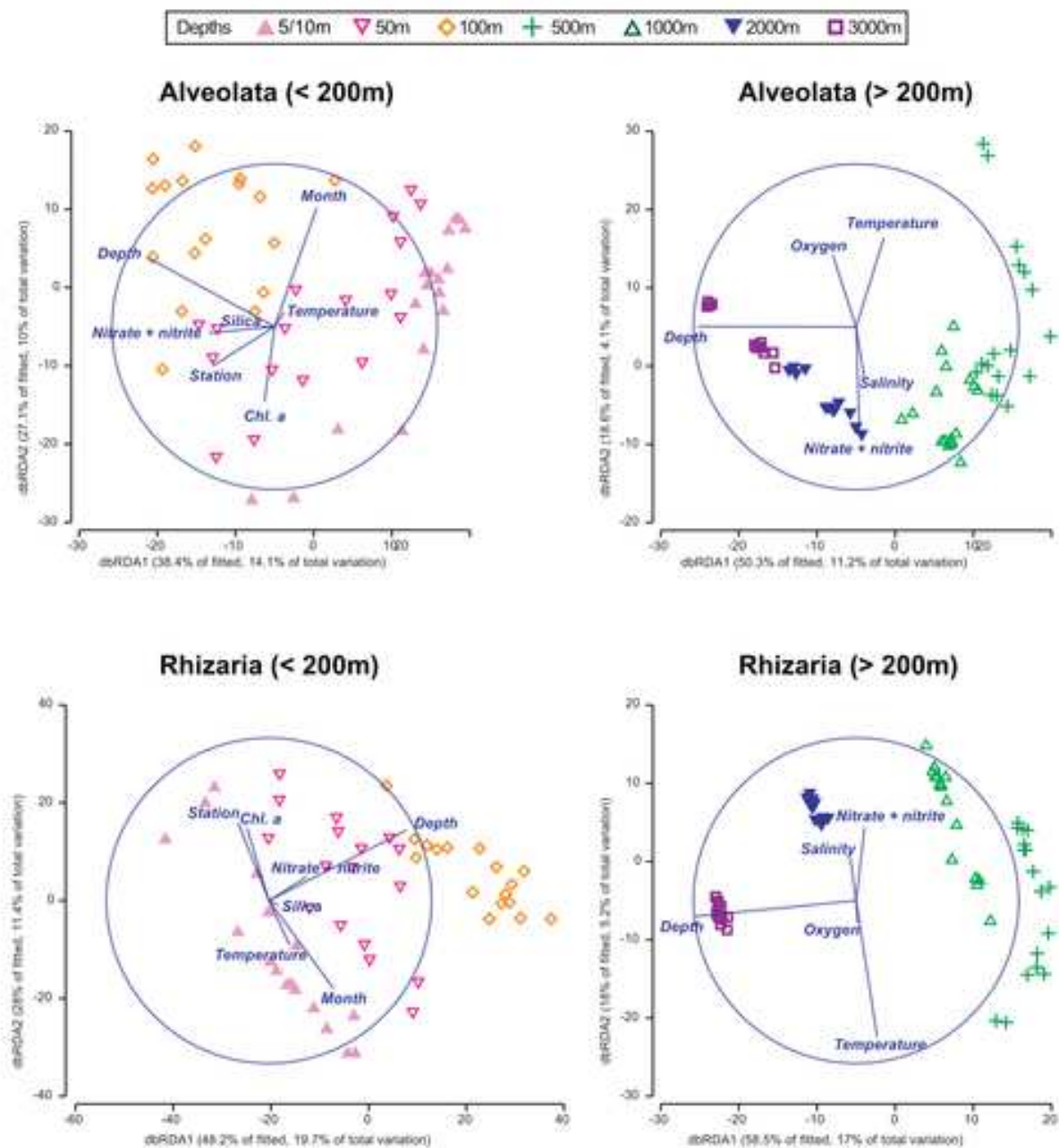


Figure 10



TABLES

Table 1. Survey cruises, sampling stations, and water depths of ~~eDNA-DNA~~ maetatabarcoding samples from the area adjacent to the Kuroshio Current

Cruise no.	Cruise dates	Sampling stations	Sampling water depths (m) ^a
SY1508	21 Aug to 2 Sep 2015	5 stations (C34, C33, C32, C31, C30)	5, 50, 100, 500, 1,000, 2,000, 3,000
SY1510	23 Oct to 4 Nov 2015	3 stations (C34, C3315, C3030)	5, 50, 100, 500, 1,000, 2,000, 3,000
SY1603	29 Feb to 9 Mar 2016	3 stations (C33345, C3310, C30)	10, 50, 100, 500, 1,000, 2,000, 3,000
SY1605	9 to 19 May 2016	3 stations (C34, C3245, C30)	10, 50, 100, 500, 1,000, 2,000 ^b , 3,000
SY1608	24 Aug to 5 Sep 2016	3 stations (C34, C33, C32)	5, 50, 100, 500, 1,000, 2,000, 3,000

^a Sampling depths up to 1,000 m at stations C34 and C3345^b Not determined at C3245

Table 2. Pairwise analysis of similarities among depths

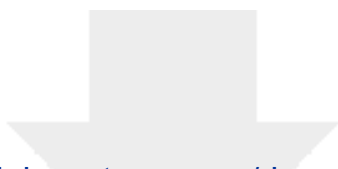
	5–10 m	50 m	100 m	500 m	1,000 m	2,000 m	3,000 m
5–10 m	-	-	-	-	-	-	-
50 m	0.128*	-	-	-	-	-	-
100 m	0.623*	0.346**	-	-	-	-	-
500 m	1**	0.999**	0.919**	-	-	-	-
1,000 m	1**	1**	0.98**	0.183**	-	-	-
2,000 m	1**	1**	0.998**	0.634**	0.394**	-	-
3,000 m	1**	1**	0.998**	0.798**	0.619**	0.221**	-

* $p < 0.001$, ** $p = 0.0001$.

Table 3. Percentage of variation explained in a distance-based multivariate linear model (DistLM) of Alveolata and Rhizaria community

Alveolata (< 200 m)		Alveolata (> 200 m)		Rhizaria (< 200 m)		Rhizaria (> 200 m)		
Variable	<i>p</i>	Variation explained (%)	<i>p</i>	Variation explained (%)	<i>p</i>	Variation explained (%)	<i>p</i>	
Depth	0.0001	11.2	0.0001	10.7	0.0001	16.5	0.0001	16.7
Temperature	0.0001	11.2	0.0001	9.6	0.0001	9.0	0.0001	14.5
Nitrate+nitrite	0.0001	13.3	0.0001	5.0	0.0001	11.3	0.0001	6.2
Salinity	0.0129	3.7	0.0001	8.1	0.0144	4.3	0.0001	12.8
Station	0.0001	5.6	0.0042	3.4	0.0086	4.8	0.09	2.6
Month	0.0001	7.5	0.4672	1.7	0.0002	7.6	0.0633	2.8
Oxygen	0.0087	3.9	0.0001	5.6	0.0003	7.2	0.0002	5.4
Position	0.0007	5.2	0.0248	2.8	0.0149	4.4	0.4255	1.7
Silica	0.0001	10.4	-	-	0.0001	7.7	-	-
Chllophyll <i>a</i>	0.0002	6.1	-	-	0.0001	8.2	-	-

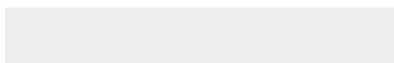
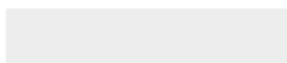


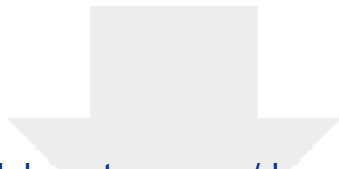


[Click here to access/download](#)

Supplementary Material

Fig_Sup2_depth_OTU_Alveo.tiff

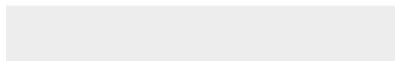
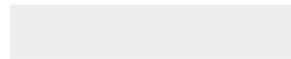


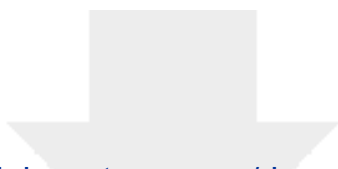


[Click here to access/download](#)

Supplementary Material

Fig_Sup3_depth_reads_Alveo.tif

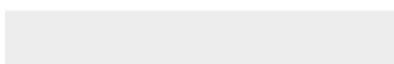


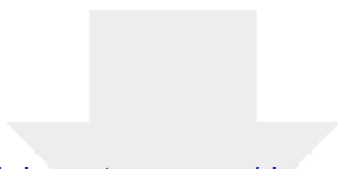


[Click here to access/download](#)

Supplementary Material

Fig_Sup4_depth_OTU_Rhiza.tiff





[Click here to access/download](#)

Supplementary Material

Fig_Sup5_depth_reads_Rhiza.tiff

